RESEARCH and

TECHNOLOGY

DEVELOPMENT

INCORPORATED

LIFE SCIENCES DIVISION

OCULAR EFFECTS OF REPETITIVE LASER PULSES

30 JUNE 1972

FINAL REPORT

Air Force Contract F41609-71-C-0018

Project 6301, Task 05, Work Unit 024

72-611

USAF School of Aerospace Medicine
Aerospace Medical Division (AFSC)
Brooks Air Force Base, Texas

Approved for public release; distribution unlimited.

93

8531 N. NEW BRAUNFELS AVE • SAN ANTONIO, TEXAS 78217

UNCLASSIFIED
Security Classification

DOCUMENT CONTROL DATA - R&D
(Security classification of title, body of abstract and indexing annotation must be entered when the overall report is classified)

1. ORIGINATING ACTIVITY (Corporate author)
Technology Incorporated, Life Sciences Division
8531 N. New Braunfels Avenue
San Antonio, Texas 78217

2a. REPORT SECURITY CLASSIFICATION
UNCLASSIFIED

2b GROUP

3 REPORT TITLE
Ocular Effects of Repetitive Laser Pulses

4. DESCRIPTIVE NOTES (Type of report and inclusive dates)
Final Report - April 1971 - June 1972

5. AUTHOR(S) (Last name, first name, initial)
Skeen, C. H.; Bruce, W. Robert; Tips, J. H., Jr.; Smith, M. Gearity; Garza, G. G.

6. REPORT DATE	7a. TOTAL NO. OF PAGES	7b. NO. OF REFS
June 1972	89	19

8a. CONTRACT OR GRANT NO.
F41609-71-C-0018
b. PROJECT NO.
6301, Task 05
c.
Work Unit 024
d.

9a. ORIGINATOR'S REPORT NUMBER(S)

9b. OTHER REPORT NO(S) (Any other numbers that may be assigned this report)

10. AVAILABILITY/LIMITATION NOTICES
APPROVED FOR PUBLIC RELEASE; DISTRIBUTION UNLIMITED

11. SUPPLEMENTARY NOTES

12. SPONSORING MILITARY ACTIVITY
USAF School of Aerospace Medicine
Aerospace Medical Division (AFSC)
Brooks Air Force Base, Texas 78235

13. ABSTRACT
An argon-ion laser was used to investigate the ocular effects of repetitive laser pulses on rhesus monkeys. The argon-ion laser was operated at a wavelength of 514.5 nm in the TEM_{00} mode. The primate eyes were irradiated by trains of pulses emitted by the argon-ion laser. The width (full-width-at-half-maximum-power) of the pulses composing the pulse trains was held constant at 10μsec and the duration of the trains was kept uniform at 0.5sec. The pulse repetition rate was used as a parameter and this parameter was varied to take on the values of 2 Hz (single pulse), 10 Hz, 100 Hz, 1 kHz and 10 kHz. Retinal burn thresholds were determined based on the 1 hr criterion for the appearance of ophthalmoscopically visible lesions. The ED50 values obtained when rhesus monkeys' eyes were irradiated with 2 Hz, 10 Hz, 100 Hz, 1 kHz and 10 kHz pulse trains were, using a probit analysis, (1.6$\pm$0.1)μJ, (0.65$\pm$0.04)μJ, (0.21$\pm$0.01)μJ, (0.155$\pm$0.007)μJ and (0.111$\pm$0.0009)μJ, respectively, with confidence limit intervals of 95%. The corresponding ED50 values using an arithmetical averaging method were (1.96$\pm$0.30)μJ, (0.64$\pm$0.08)μJ, (0.22$\pm$0.02)μJ, (0.22$\pm$0.02)μJ, (0.15$\pm$0.01)μJ, (0.12$\pm$0.01)μJ, respectively. Comparison of the thresholds obtained using the pulse trains with the threshold for the 2 Hz (single pulse) case, it is concluded that a cumulative effect exists for the pulses in the pulse trains. This cumulative effect is by definition that the otherwise subthreshold pulses, based on the 1 hr criterion, work in concert to produce retinal lesions.

DD FORM 1 JAN 64 1473

UNCLASSIFIED
Security Classification

14. KEY WORDS	LINK A		LINK B		LINK C	
	ROLE	WT	ROLE	WT	ROLE	WT
Argon-Ion laser; thermal injury; retinal burns; repetitive pulse lasers; rhesus monkey; laser safeguards; laser safety standards						

INSTRUCTIONS

1. ORIGINATING ACTIVITY: Enter the name and address of the contractor, subcontractor, grantee, Department of Defense activity or other organization *(corporate author)* issuing the report.

2a. REPORT SECURITY CLASSIFICATION: Enter the overall security classification of the report. Indicate whether "Restricted Data" is included. Marking is to be in accordance with appropriate security regulations.

2b. GROUP: Automatic downgrading is specified in DoD Directive 5200.10 and Armed Forces Industrial Manual. Enter the group number. Also, when applicable, show that optional markings have been used for Group 3 and Group 4 as authorized.

3. REPORT TITLE: Enter the complete report title in all capital letters. Titles in all cases should be unclassified. If a meaningful title cannot be selected without classification, show title classification in all capitals in parenthesis immediately following the title.

4. DESCRIPTIVE NOTES: If appropriate, enter the type of report, e.g., interim, progress, summary, annual, or final. Give the inclusive dates when a specific reporting period is covered.

5. AUTHOR(S): Enter the name(s) of author(s) as shown on or in the report. Enter last name, first name, middle initial. If military, show rank and branch of service. The name of the principal author is an absolute minimum requirement.

6. REPORT DATE: Enter the date of the report as day, month, year, or month, year. If more than one date appears on the report, use date of publication.

7a. TOTAL NUMBER OF PAGES: The total page count should follow normal pagination procedures, i.e., enter the number of pages containing information.

7b. NUMBER OF REFERENCES: Enter the total number of references cited in the report.

8a. CONTRACT OR GRANT NUMBER: If appropriate, enter the applicable number of the contract or grant under which the report was written.

8b, 8c, & 8d. PROJECT NUMBER: Enter the appropriate military department identification, such as project number, subproject number, system numbers, task number, etc.

9a. ORIGINATOR'S REPORT NUMBER(S): Enter the official report number by which the document will be identified and controlled by the originating activity. This number must be unique to this report.

9b. OTHER REPORT NUMBER(S): If the report has been assigned any other report numbers *(either by the originator or by the sponsor)*, also enter this number(s).

10. AVAILABILITY/LIMITATION NOTICES: Enter any limitations on further dissemination of the report, other than those imposed by security classification, using standard statements such as:

(1) "Qualified requesters may obtain copies of this report from DDC."

(2) "Foreign announcement and dissemination of this report by DDC is not authorized."

(3) "U. S. Government agencies may obtain copies of this report directly from DDC. Other qualified DDC users shall request through

_____."

(4) "U. S. military agencies may obtain copies of this report directly from DDC. Other qualified users shall request through

_____."

(5) "All distribution of this report is controlled. Qualified DDC users shall request through

_____."

If the report has been furnished to the Office of Technical Services, Department of Commerce, for sale to the public, indicate this fact and enter the price, if known.

11. SUPPLEMENTARY NOTES: Use for additional explanatory notes.

12. SPONSORING MILITARY ACTIVITY: Enter the name of the departmental project office or laboratory sponsoring *(paying for)* the research and development. Include address.

13. ABSTRACT: Enter an abstract giving a brief and factual summary of the document indicative of the report, even though it may also appear elsewhere in the body of the technical report. If additional space is required, a continuation sheet shall be attached.

It is highly desirable that the abstract of classified reports be unclassified. Each paragraph of the abstract shall end with an indication of the military security classification of the information in the paragraph, represented as *(TS)*, *(S)*, *(C)*, or *(U)*.

There is no limitation on the length of the abstract. However, the suggested length is from 150 to 225 words.

14. KEY WORDS: Key words are technically meaningful terms or short phrases that characterize a report and may be used as index entries for cataloging the report. Key words must be selected so that no security classification is required. Identifiers, such as equipment model designation, trade name, military project code name, geographic location, may be used as key words but will be followed by an indication of technical context. The assignment of links, rules, and weights is optional.

OCULAR EFFECTS OF REPETITIVE LASER PULSES

FINAL REPORT

30 JUNE 1972

C. H. Skeen, Ph. D., W. Robert Bruce,
J. H. Tips, Jr., M. S. , M. Gearity Smith, B S., G. G. Garza

Air Force Contract F41609-71-C-0018

Project 6301, Task 05, Work Unit 024

Approved by:

James V. Benedict, Ph.D.
Manager, San Antonio Branch
Life Sciences Division

FOREWORD

The cooperation of the Vivarium personnel at Brooks Air Force Base, notably Sgts. E. L. Hendrix, F. W. Smith and A. E. Wiedeman, was outstanding and greatly appreciated. Special thanks are extended to Dr. Robert W. Ebbers for his assistance as the contract monitor, to Dr. Ebbers, Dr. Irving L. Dunsky and Mr. E. O. Richey for many helpful consultations throughout this study and to Mr. Richard McNee for calling to our attention a possible fundamental difficulty in applying the probit analysis to retinal burn data.

The work in the animal holding facilities and in the animal preparations at Technology Incorporated done by Mr. Robert Neish and Mr. Peter Herrera, and the photographic service supplied by Mr. Richard Johnson was most helpful as was the art work done by Mr. Hector Lizcano.

Our appreciation is hereby expressed to Mrs. Linda Anderson and Mrs. Melba Robb for typing this final report and for their secretarial support throughout this program.

Last, but far from least, our thanks are accorded to Dr Ralph G. Allen, Dr. J. V. Benedict and Dr. Martin M. Mainster for numerous conferences which led to our understanding and to our interpretation of our experimental results.

LIST OF FIGURES

LIST OF TABLES

TABLE OF CONTENTS

1. INTRODUCTION

Lasers are coherent, highly collimated, nearly monochromatic and very intense light sources. Laser light is uniquely hazardous to the skin and eyes of personnel because of the intensity and collimation of the beam. The eye is particularly vulnerable to the laser light which it transmits efficiently (visible and near infrared wavelengths). The visible and near infrared laser light can be quite low in intensity and still be very hazardous because the fluence (energy per unit area) is about a factor of 10^5 greater at the retina than at the cornea.

It is required that lasers be used following realistic safeguard procedures. Because of the complexity of the phenomena involved, laser induced chorioretinal effects cannot be determined theoretically with the precision required for establishing realistic safeguards. Laser safeguard procedures are established to assure that ocular exposures of the personnel involved are equal to or less than some prescribed values referred to as permissible exposure levels (PEL). These PEL are based on retinal burn thresholds determined from ocular effects experiments in which rhesus monkeys are exposed to light from a laser operating under specified conditions. These thresholds are translated to humans by using the an arbitrary variability factor between these species.

The complexity of laser induced chorioretinal effects can be appreciated when it is recognized that these effects depend upon many parameters such as (1) the laser wavelength, (2) the laser beam divergence, (3) the laser

beam energy distribution, (4) the pupil size, (5) the accommodation, (6) the direction in which the laser light beam is viewed, (7) the light absorption and the thermal transfer properties of the eye and (8) the body temperature. A research program in which each of these parameters is varied systematically to determine the corresponding retinal burn thresholds would require a very large and impractical number of experiments to be performed. This impractical situation required laser safety experts to search for ways to limit the number of experiments needed to obtain reliable data for the establishment of realistic laser safeguard procedures. This search led logically to the performance of credible "worst-case" experiments using laser light at a given wavelength. Experiments now being performed are "worst-case" in the sense that (1) the primate eyes involved are corrected for refractive errors, chromatic aberrations and are relaxed to focus at infinity and (2) the laser beam divergence is chosen, within practical limits, so that the beam is focused into a "smallest-size-spot" at the retina. Thus, retinal burn thresholds are lower for this "worst-case" than for any other condition.

The laser beam divergence is related to the mode of the energy distribution in its associated wavefront. The mode of the energy distribution is written symbolically by using the notation TEM_{ij} where the subscripts i and j refer to the order of the modes and correspond to the nodes in the transverse electromagnetic field inside the laser cavity. The higher the order of the mode, the more complex the energy distribution and the larger the laser beam divergence.

The TEM_{00} mode is the lowest order mode for a laser and corresponds (1) to a Gaussian energy distribution in the wavefront and (2) to a diffraction limited beam from the laser. The diameter of the "smallest-size-spot" at the retina can be approximated by the product of the focal length of the primate eye and the laser beam divergence (full angle, i.e. twice the angular spread of the Airy disc). Thus, in the "worst-case" retinal burn threshold experiments, lasers operating in the TEM_{00} mode are used. Allen and coworkers verified[1] that the smaller the spot size the lower the retinal burn threshold using a white light source; and, this was verified[2] later by King and Geereats using a laser light source.

Clarke [3] and Sliney [4] discuss problems relevant to quantifying laser ocular hazards and the development of laser safety criteria as well as reviewing most of the laser retinal burn threshold experiments done prior to 1970. Vassiliadis [5] discusses most of the problems arising in attempts to predict theoretically the values for retinal burn thresholds.

Recent experiments relate almost exclusively to the "worst-case" conditions. One document [6] contained a discussion of results of previous experiments and reported new results for a Nd^{3+}-YAG laser operating in the TEM_{00} mode at a wavelength of 1060 nm. A brief summary of "worst-case" experiments at visible laser wavelengths is presented in the following

paragraphs.

Dunsky and Lappin reported [7] results for retinal burn thresholds for primates obtained using a krypton laser operating at a wavelength of 568.2 nm in the TEM_{00} mode with a beam divergence of 8×10^{-4} radians. Dunsky and Lappin carefully avoided irradiating the macular region of the primate eyes and made exposures having durations ranging from 16×10^{-3} sec to 0.5 sec. Based on retinoscopic and ophthalmoscopic examinations, Dunsky and Lappin corrected the primates' vision for chromatic abberations and refractive errors by using ophthalmic lenses. Retinal burns were observed using the 1 hr criterion for the detection of ophthalmoscopically visible lesions.

Bresnick and coworkers used [8] an argon-ion laser operating at a wavelength of 514.5 nm in the TEM_{00} mode with a beam divergence of 7×10^{-4} radians to determine retinal burn thresholds for primates. Bresnick corrected the vision of the primates for chromatic aberrations and refractive errors using ophthalmic lenses. All irradiations were made in the macular region of the primate eyes using exposures with durations, in turn, of 12×10^{-3} sec, 70×10^{-3} sec, 0.125 sec and 1.0 sec. They used a 1 hr criterion for the observation of lesions with an ophthalmoscope. In addition, Bresnick compared retinal burn thresholds determined using the ophthalmoscope observations with retinal burn thresholds obtained

using a histopathological technique. The results using the histopathologic technique were below those using the ophthalmoscope consistently by 20 to 25 percent.

Ham and colleagues employed[9] a He-Ne laser operating at a wavelength of 632.8 nm in the TEM_{00} mode with a beam divergence of 7×10^{-4} radians to determine retinal burn thresholds for rhesus monkey eyes. No mention was made of correcting the primate eyes for chromatic aberrations and refractive errors. All exposures of monkeys were made in the parafovea; and, the exposure durations ranged from 15×10^{-3} sec to 1 sec. Their results were based on the 1 hr criterion for the appearance of ophthalmoscopically visible lesions. Ham and coworkers estimated that the spot diameters for their "worst-case" experiments ranged from 50 μm to 200 μm. Moreover, they pointed out the problem of using an ophthalmoscope to observe retinal lesions smaller in diameter than 50 μm owing to the poor visual contrast and the existence of retinal inhomogeneities which are about 50 μm in diameter or smaller.

Frisch and coworkers reported[10] results for both a long-pulsed argon-ion laser and a Q-switched ruby laser. Each laser was operated in the TEM_{00} mode. The argon-ion laser was operated at a wavelength of 514.5 nm and the ruby laser was operated at a wavelength of 694.3 nm. The beam divergence was 7×10^{-4} radians and 1.0×10^{-3} radians for

these two systems, respectively. Exposure durations were 12×10^{-3} sec and 0.125 sec for the argon-ion laser and 30×10^{-9} sec for the Q-switched ruby laser. The rhesus monkey eyes were corrected for refractive errors and chromatic aberrations. Using histopathological techniques, they compared suprathreshold lesions produced in turn by the two lasers. They found that the Q-switched laser always produced massive retinal damage when monkey eyes were irradiated at levels about 10 to 15 times threshold. This compared with extensive retinal damage with occasional sub-retinal bleeding for irradiations with the long-pulsed argon-ion laser when the threshold was exceeded by a factor of 10 to 15. Hence, they concluded that miscalculations of retinal burn thresholds could lead to far more catastrophic results with a Q-switched laser than with a long-pulsed laser.

Vassiliadis and colleagues reported [11] results for the ocular effects of a He-Ne laser and an argon-ion laser. Each laser was operated in the TEM_{00} mode with a beam divergence of 7.0×10^{-3} radians. The He-Ne laser was operated at a wavelength of 632.8 nm and exposure durations were 13.5×10^{-3} sec and 80×10^{-3} sec. The argon-ion laser was operated in turn at a wavelength of 514.5 nm and at a wavelength of 488.0 nm. The durations for the argon-ion exposures were 1.5×10^{-3} sec, 4.4×10^{-3} sec, 13.5×10^{-3} sec, 80×10^{-3} sec, and 0.205 sec.

They made exposures in the macular and paramacular regions of eyes that were corrected for refractive errors and chromatic aberrations using ophthalmic lenses. Their observations were based upon the 1 hr criterion for the appearance of ophthalmoscopically visible lesions.

These experiments were reviewed here to show that not all the "worst-case" experiments involved the most sensitive part of the retina (the macular region) and to show that the eyes were not always corrected to give the smallest diameter spot. This will be kept in mind later in this report when our results are compared with those obtained with these other studies.

This brief review of "worst-case" experiments reveals that retinal burn thresholds depend upon the exposure duration. If these thresholds are expressed in terms of the energy per pulse incident on the cornea, then the thresholds are lower the shorter the exposure duration. In addition, this brief review shows that the ocular effects for visible laser light are documented rather well for "worst-case" experiments for exposure durations on the interval ranging from 1.5×10^{-3} sec to 1 sec; and, these ocular effects experiments are practically non-existent for exposures having durations of 1.0×10^{-3} sec or shorter.

Finally, this review shows that no previous experiments were performed to determine the ocular effects of repetitive pulse lasers operating

at visible wavelengths.

Some laser systems being used by Air Force personnel operate at visible wavelengths and in the repetitive pulse mode. It is expected such systems will come into greater use in the future. Since it is required that these systems be operated safely, "worst-case" experiments are needed to obtain the necessary information to establish safeguards for these systems. Consequently, the work performed on the program discussed herein was done to furnish some initial information for use in establishing the safety criteria. The results of this work are reported in the following sections.

2. EXPERIMENTAL PROCEDURES

2.1 Laser System

A Coherent Radiation, Inc. model 52G-A argon-ion laser system was used in the experiments. A photograph of this system, with a cover removed, is shown in Figure 1. It was operated (see Appendix A for details) at a wavelength of 514.5 nm in the TEM_{00} mode. Measured between the $1/e^2$ points in the cylindrically symmetric radial energy distribution in the wavefront, the beam diameter was 1.5 mm. The beam divergence (full angle) was 8×10^{-4} radians. The maximum cw laser power output was 1.3 watts.

The cw laser power of this system was modulated with a Coherent Radiation, Inc. model 462 acoustical-optical shutter. This modulation was performed so that the laser emitted single pulses with full-width-at-half-maximum-power (FWHMP) of 10 μsec. In addition, this laser system was modulated to emit pulse trains. The FWHMP of the pulses composing a train was held fixed at 10 μsec, the duration of the trains was held constant at 0.5 and the pulse repetition rate was used as a parameter. The pulse repetition rate was varied and took on the values of 10 Hz, 100Hz, 1KHz and 10kHz.

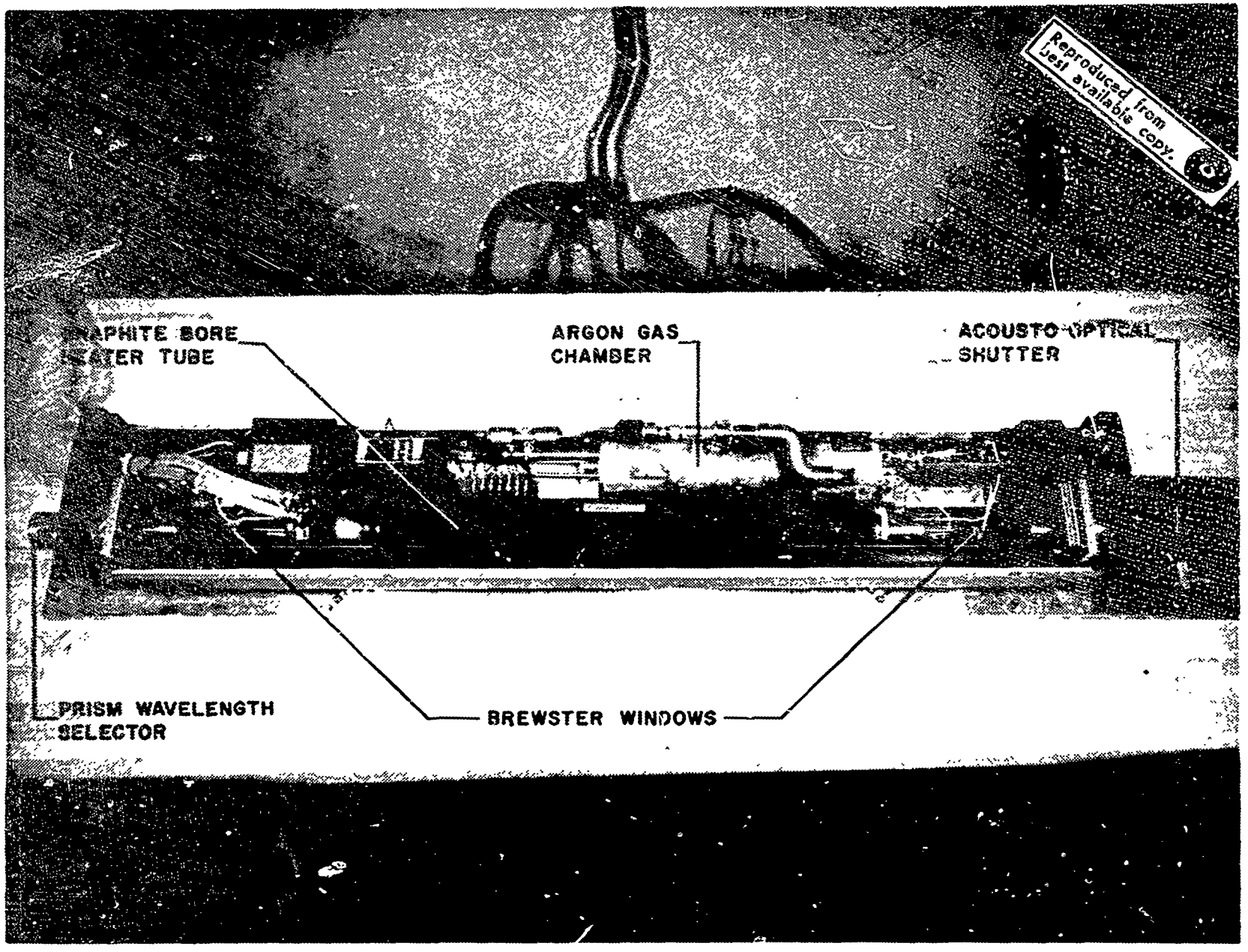

Figure 1 Argon-Ion Laser with Top Cover Removed

2.2 Laser System Calibrations

The waveforms of the emitted pulses and pulse trains were detected with an EG&G model SGD-100 diffuse-silicon photodiode in conjunction with a Tetronix model 555 dual-beam oscilloscope. The photodiode had a reverse bias of 30 volts.

The waveforms detected by the photodiode-scope array were calibrated (see Appendix B for details) to determine (1) the instantaneous power of the pulses and (2) the energy of the pulses. These calibrations were performed using two detectors which had calibrations traceable to NBS values. One of these detectors was a HADRON/TRG model 100 ballistic thermopile in conjunction with a Keithley model 150 B microvolt meter and the other detector was a Coherent Radiation, Inc. model 201 power meter. Using these calibrations, it was demonstrated that the photodiode, with the reverse bias of 30 volts, responded within its linear dynamic range for every irradiation performed in this study. These calibrations were performed daily and the energy and/or the power per pulse was determined for every irradiation done in the experiments reported in this document.

2.3 Primate Housing and Preparations

Macaca Mulattas (rhesus monkeys) were used as subjects in the

experiments. These primates were kept in the animal housing facility at Technology Incorporated. The animal housing facility at the Life Sciences Division of Technology Incorporated had a carefully controlled environment where the primates were housed individually in modern stainless steel cages. The animals and facility are maintained in accordance with the "Guide for Laboratory Animals, Facilities and Care" as published by the National Academy of Sciences-National Research Council. Regular inspections were made by a representative of the U. S. Department of Agriculture, Agricultural Research Service, Animal Health Division.

Primate preparation for various experimental procedures were carried out in the animal surgery suite. The surgery suite consisted of a preparation room, a scrub room, and an operating room. Initial preparations (e.g., sedation, pupil dilation, body weight determination) were performed in the surgery preparation room. The operating room was modern and equipped for the most sophisticated experimental preparations and procedures.

On the day prior to the retinal irradiations of a primate, atropine sulfate, 1% ophthalmic ointment was introduced into the conjunctival sac. This procedure was utilized to give maximum pupillary dilation.

Just prior to the retinal irradiations, the primate was tranquilized with phencyclidine hydrochloride (Sernylan) 20 mg/cc, IM. The dosage employed was 1 mg/Kg of body weight. Then an anesthetizing procedure was started, by introducing a 19 gauge intravenous catheter into a posterior superficial vein in a leg. Initially 0.5 cc of sodium pentobarbital, 50 mg/cc, was administered by way of the intra-catheter; and, smaller increments were injected as necessary to maintain deep anesthesia. Lacrimation was usually suppressed by anesthesia; therefore, the eye was frequently irrigated with normal saline or artificial tears to preserve corneal transparency.

Following anesthetization, thorough ophthalmoscopic and slit-lamp examinations of the eyes were performed. Following the slit-lamp examination, the refractive error for each eye of the primate was determined with a retinoscope. Refractive errors for chromatic aberration were determined with a retinoscope in conjunction with band-pass filters at 475, 517, and 610 nm. The corrective lens necessary at a wavelength of 475 nm was -0.5 diopter, at 517 nm it was -0.25 diopter and at 610 nm it was +0.25 diopter. Based on these results, it was estimated that the corrective lens for chromatic aberration at 514.5 nm was -0.25 diopter [12][13]. The necessary corrective lens was used for each rhesus monkey eye irradiated.

Finally, during the irradiations, a 402 rectal probe and Yellow Springs model 72 Tele-Thermometer were used at all times to monitor primate core temperature.

2.4 Retinal Irradiations

The argon-ion laser, salient features of the energy delivery system and the arrangement used in the irradiation of the primate eyes are shown in Figure 2. A sequence of events during a retinal irradiation procedure was as follows. The cornea of an eye of an anesthetized primate was cleared by the operator and a site in the macular area selected. The cross-hairs of an ophthalmoscope light were positioned so as to intersect at the chosen site. A solenoid on the ophthalmoscope was energized and the "pop-up" mirror came into place. Then an electronic signal in the form of a voltage pulse was generated internally at the Q-switch controller box causing a single 10 μsec pulse or a single pulse train to be emitted by the laser and focused onto the retina with the primate eye's own optics.

"Marker burns", which served as fiducial points, were placed at the corners of a square with 1.5 mm diagonal centered on the fovea. Up to 26 independent irradiations including the "marker burns" were placed in the macular region. All exposures, with the exception of the "marker burns" were placed at random in the macula.

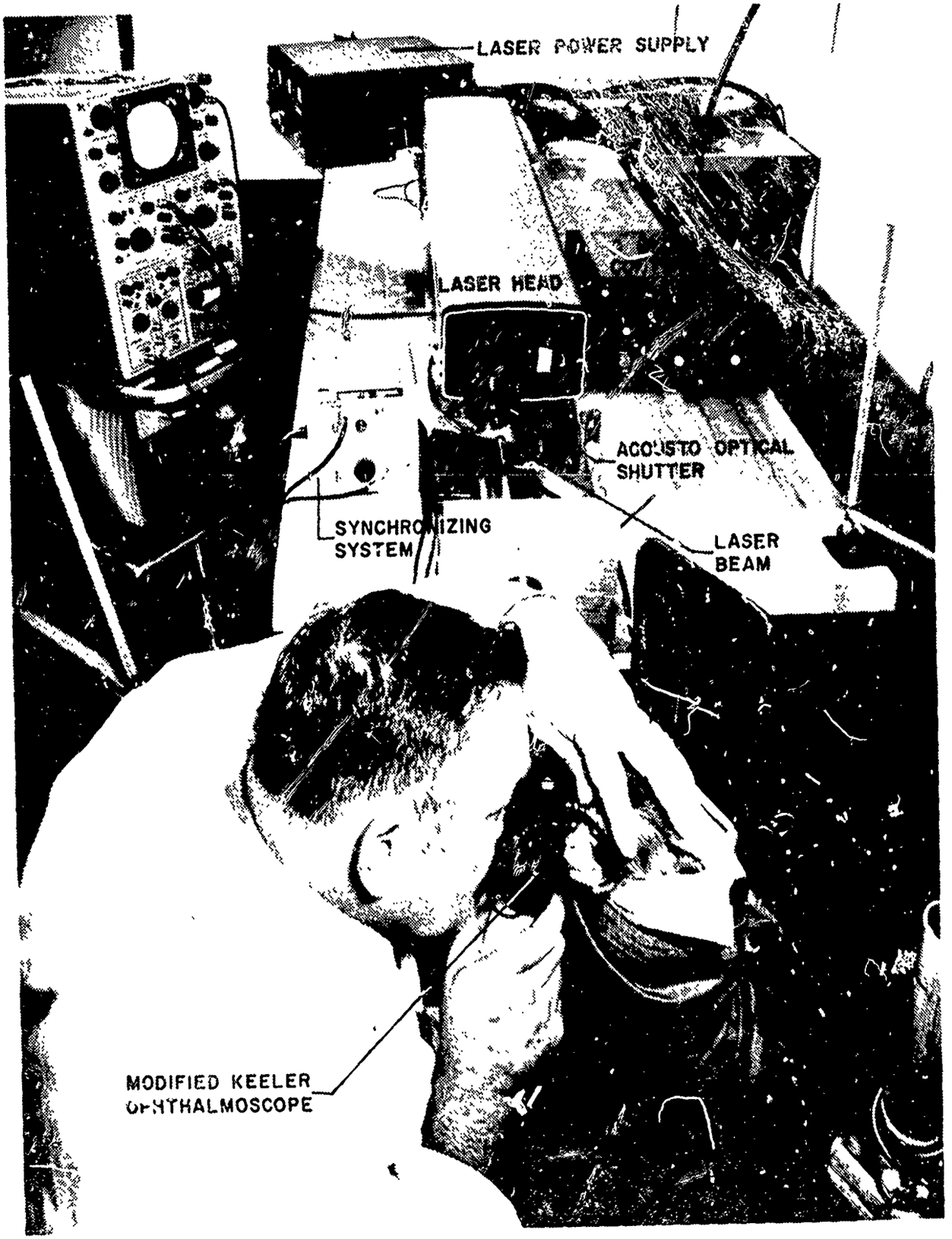

Figure 2 Laser System and Ancillary Equipment for Retinal Irradiation

Fundus photographs were taken after some exposures. An example of one of these photographs is shown in Figure 3. A schematic diagram of the macular region typical of a rhesus monkey fundus is shown in Figure 4. A pattern of the irradiation sites used is shown in Figure 5. This irradiation pattern was varied for each eye irradiated. The power of the laser light at the cornea was varied in turn for the different retinal irradiations. The irradiated sites were observed periodically at time intervals up to an hour subsequent to the irradiations and a record made as to whether or not a lesion appeared. From these data, a retinal burn threshold was determined for each eye.

Some suprathreshold lesions produced in the determination of a typical retinal burn threshold are shown in Figure 6.

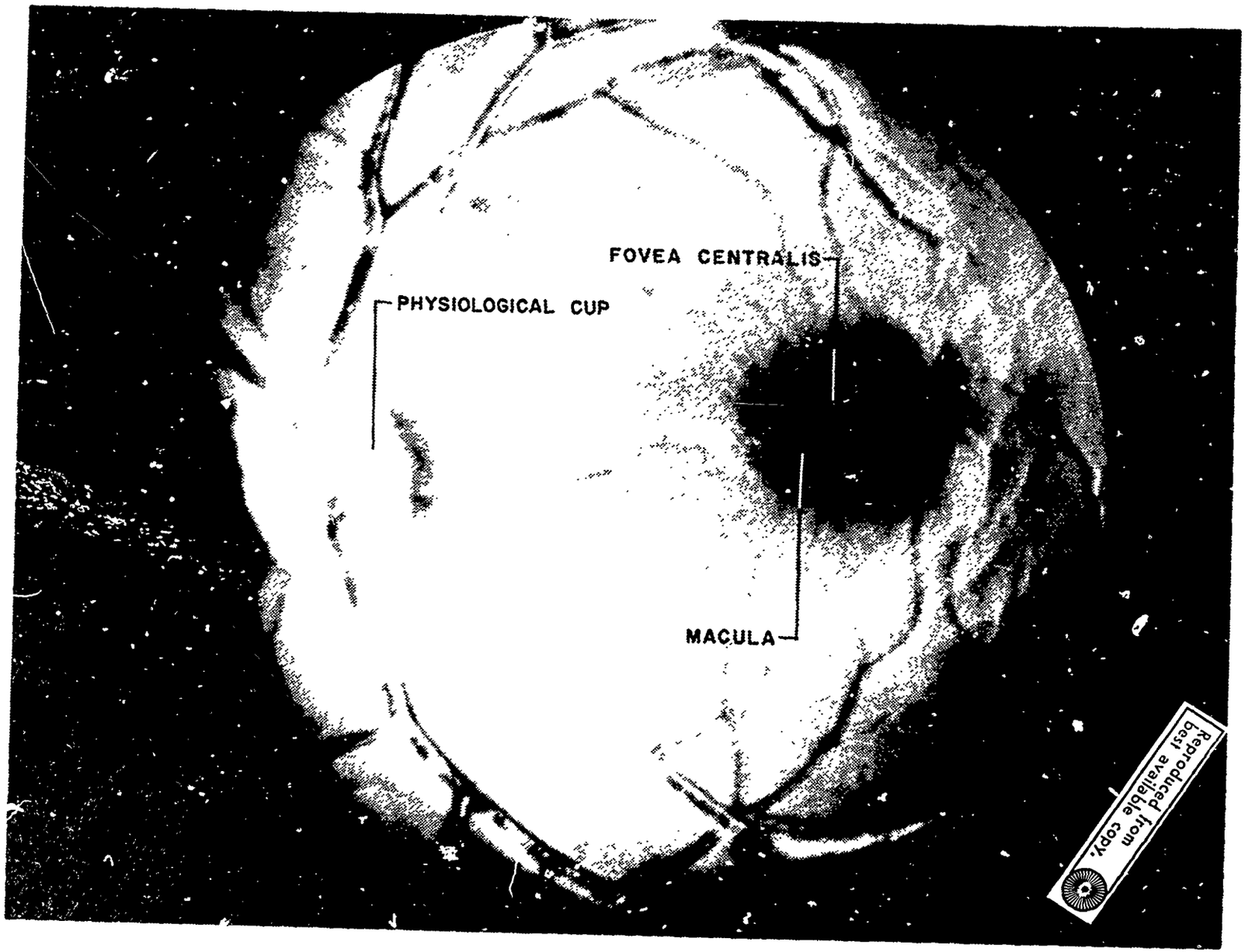

Figure 3 Typical Fundus of a Macaca Mulatta

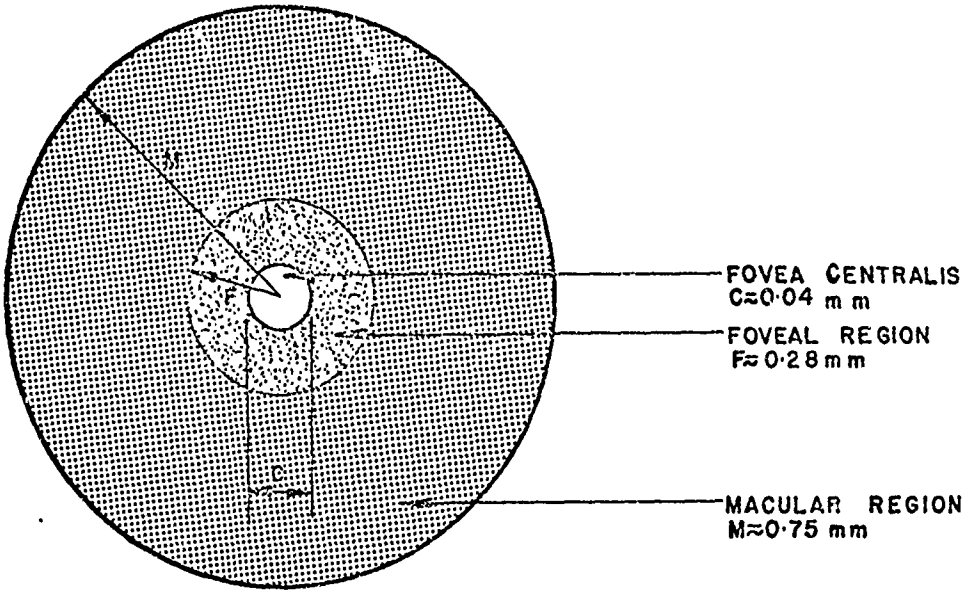

Figure 4. Schematic Diagram of the Macular Region of the Macaca Mulatta (rhesus monkey) Fundus

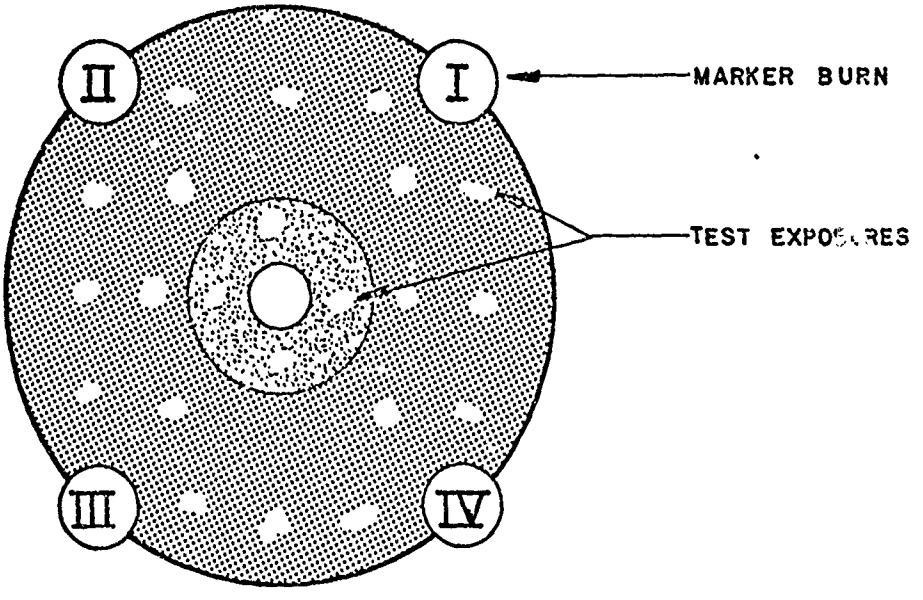

Figure 5. Diagram Showing "Marker Burn" Locations and Typical Irradiation Pattern

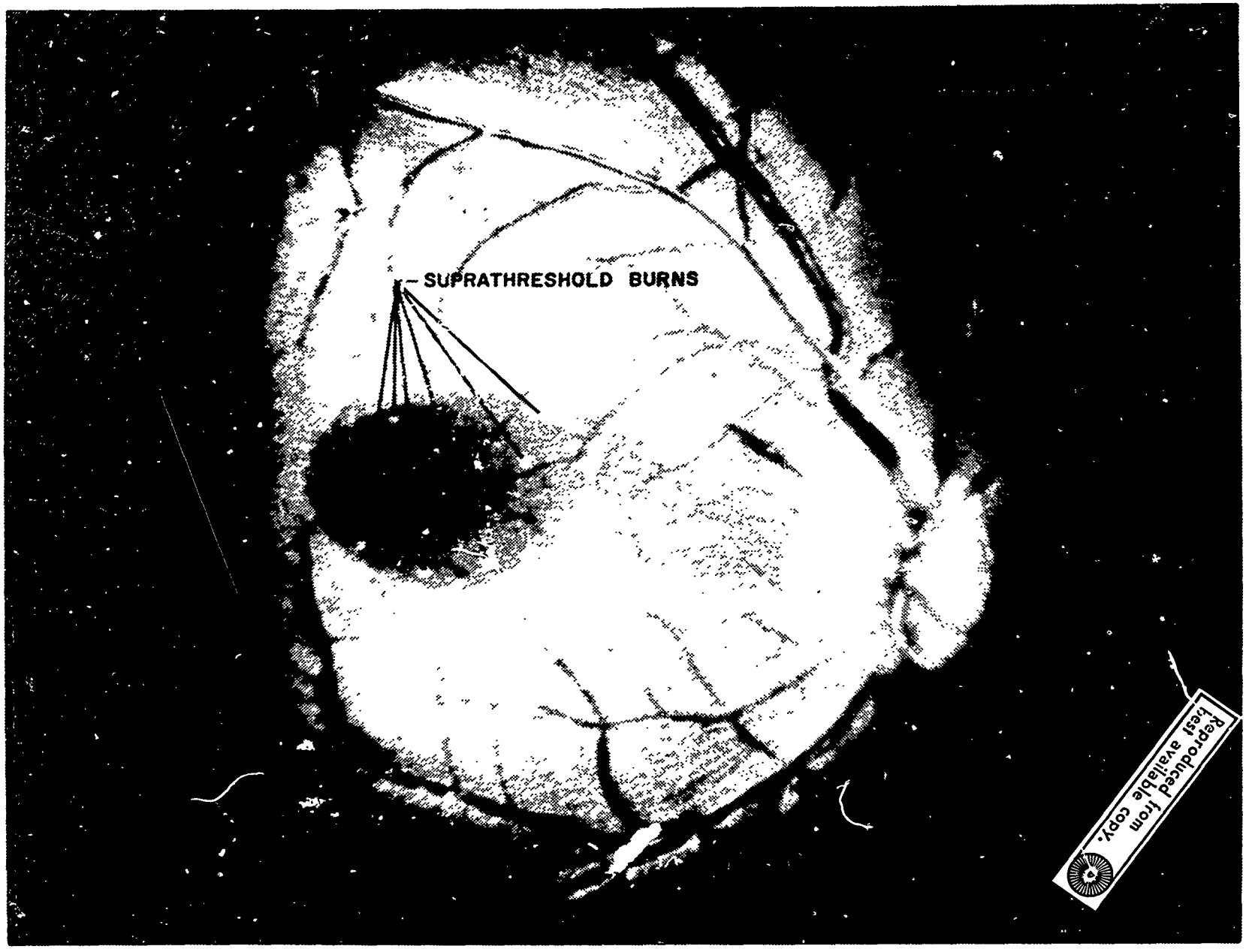

Figure 6 Fundus Photograph Showing Suprathreshold Retinal Burns

3. EXPERIMENTAL RESULTS

3.1 Single Pulse Experiments

A waveform typical of those used in the irradiation of primate eyes with the single 10 μsec pulses is shown in Figure 7. Typical data like those secured to determine the retinal burn thresholds for 30 primate eyes are shown in Table I. The retinal burn thresholds obtained for the 30 eyes are shown in Table II. Data like those displayed in Table I were analyzed using the probit method[14] (see Appendix C for details) and the results for the retinal burn probability versus the energy per pulse incident on the primate corneas are shown in Figure 8.

3.2 Pulse Train Experiments

Primate eyes were irradiated with trains of the 10 μsec pulses having waveforms like that displayed in Figure 7. As mentioned previously in this report the durations of the trains of the 10 μsec pulses was held constant and the pulse repetition rate was used as a parameter. This parameter was varied and took on the values of 10 Hz, 100 Hz, 1 kHz and 10 kHz. Typical retinal burn data for these four trains are shown in Tables III - VI, respectively; and the corresponding retinal burn thresholds obtained are shown in Tables VII-X, respectively. Data like those in Tables III-VI were analyzed using

the probit technique. The results obtained for the retinal burn probability versus the energy per pulse for the 10 Hz, 100 Hz, 1 kHz and 10 kHz pulse trains are shown in Figures 9-12, respectively.

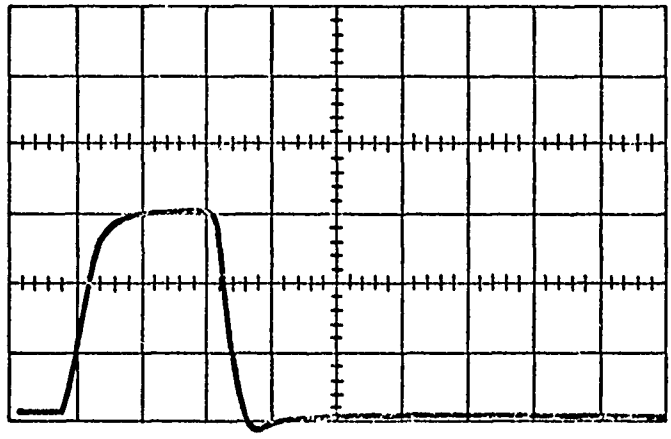

Figure 7. Tracing of a Typical Single 10 μ sec Pulse at a Wavelength of 514.5 nm (the Sweep Rate was 5 μ sec/cm.

Table I. A Sample of Retinal Burn Data for Single 10 μsec Exposures of a Rhesus Monkey Eye to the 514.5 nm Laser Light (Eye No.208)

Exposure	Energy μj	Burn/No Burn
		Burn
1	4.00	Burn
2	3.71	Burn
3	3.78	Burn
4	3.90	Burn
5	1.89	Burn
6	1.76	Burn
7	1.38	No Burn
8	1.54	Burn
9	1.70	Burn
10	1.50	Burn
11	1.42	No Burn
12	1.84	Burn
13	1.54	Burn
14	1.59	Burn
15	1.59	No Burn
16	1.74	Burn
17	1.54	Burn
18	1.28	No Burn
19	1.43	No Burn
20	1.28	No Burn
21	.97	No Burn
22	.90	No Burn
23	.77	No Burn
24	.82	No Burn
25	.79	No Burn

Table II. Retinal Burn Thresholds for Rhesus Monkeys' Eyes for Exposures to Single 10 μsec Pulses from Argon-Ion Laser Operating at a Wavelength of 514.5 nm in the TEM_{00} Mode.

Eye No.	Energy/Pulse μJ
184	4.44
185	2.23
186	1.70
187	2.72
188	2.49
189	2.21
190	1.28
191	3.48
192	2.34
193	3.06
194	2.25
195	2.57
196	1.41
197	1.79
198	1.45
199	2.07
200	0.890
201	1.66
202	1.60
203	3.07
204	1.61
205	1.29
206	2.00
207	2.07
208	1.47
209	1.48
210	0.870
211	0.720
212	1.14
213	1.37

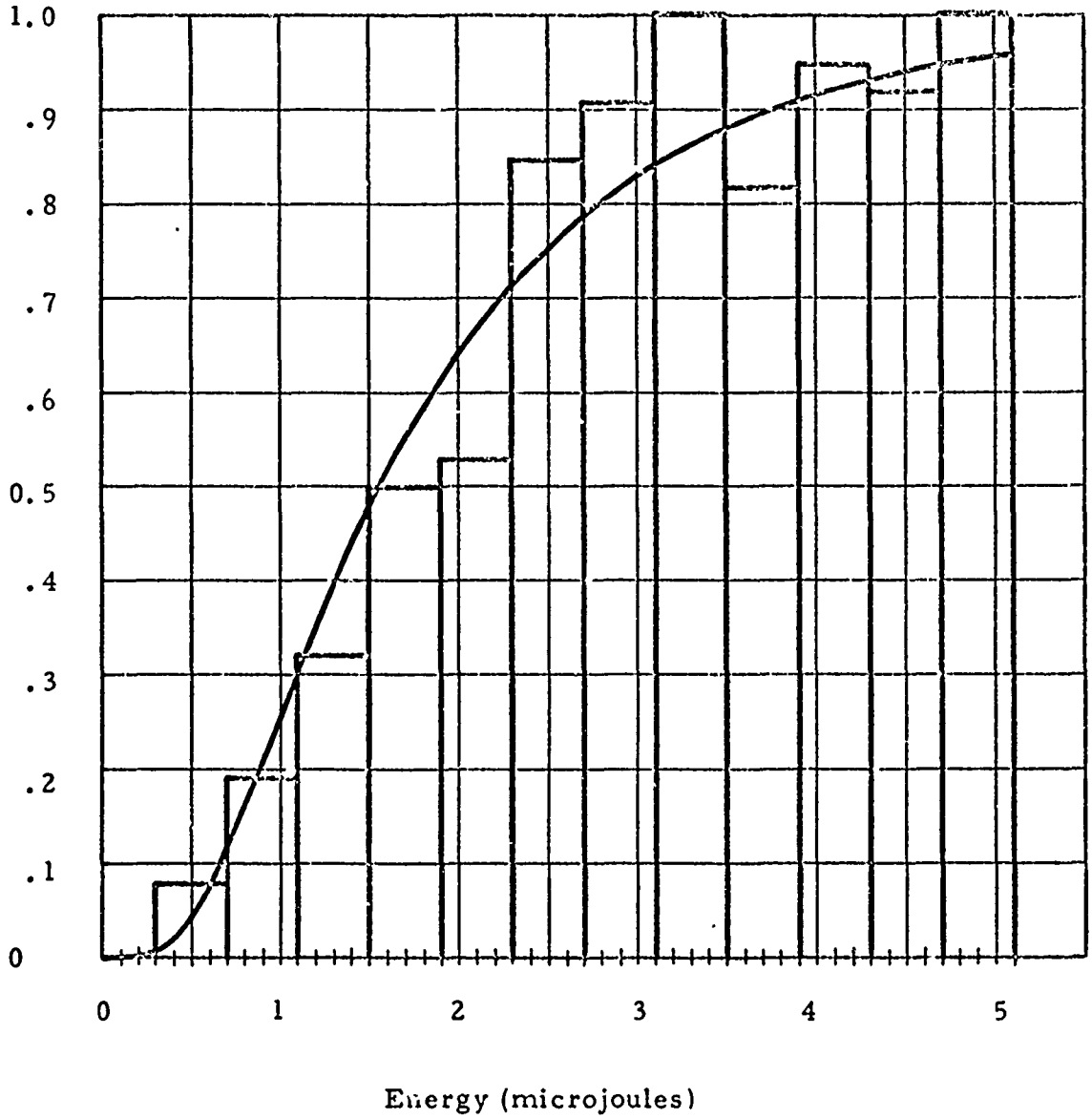

Figure 8. Retinal Burn Probability versus Energy of the Single 10μsec Laser Pulses at a wavelength of 514.5 nm. (30 eyes)

Table III. Typical Retinal Burn Data for the 10Hz Pulse Trains. (Eye No. 216)

Exposure Number	Energy per 10 μ sec pulse μ J	Burn/No Burn
1	5.93	Burn
2	4.79	Burn
3	3.53	Burn
4	2.39	Burn
5	2.05	Burn
6	1.82	Burn
7	1.65	Burn
8	1.43	Burn
9	1.20	Burn
10	0.97	No Burn
11	0.73	No Burn
12	0.50	No Burn
13	0.41	No Burn

Table IV. Typical Retinal Burn Data for the 100Hz Pulse Trains (Eye No. 267)

Exposure Number	Energy per 10 μ sec pulse μJ	Burn/No Burn
1	1.10	Burn
2	.627	Burn
3	.627	Burn
4	.403	Burn
5	.381	Burn
6	.381	Burn
7	.347	Burn
8	.325	Burn
9	.307	Burn
10	.280	Burn
11	.237	Burn
12	.217	Burn
13	.157	No Burn
14	.146	No Burn
15	.121	No Burn
16	.099	No Burn
17	.072	No Burn

Table V.. Typical Retinal Burn Data for the 1kHz Pulse Trains (Eye No. 274)

Exposure Number	Energy per 10μ sec pulse μJ	Burn/No Burn
1	.634	Burn
2	.429	Burn
3	.378	Burn
4	.327	Burn
5	.276	Burn
6	.215	Burn
7	.194	Burn
8	.170	No Burn
9	.143	No Burn
10	.127	No Burn
11	.106	No Burn
	.082	No Burn
13	.063	No Burn
14	.045	No Burn

Table VL Typical Retinal Burn Data for the 10kHz Pulse Trains (Eye No. 324)

Exposure Number	Energy per 10μ sec pulse μ J	Burn/No Burn
1	1.39	Burn
2	.98	Burn
3	.73	Burn
4	.52	Burn
5	.49	Burn
6	.43	Burn
7	.33	Burn
8	.27	Burn
9	.19	Burn
10	.12	Burn
11	.11	No Burn
12	.085	No Burn
13	.070	No Burn
14	.047	No Burn
15	.024	No Burn
16	.011	No Burn
17	.009	No Burn

Table VII. Retinal Burn Thresholds for Rhesus Monkeys' Eyes for Exposures to Trains of 10 μsec Pulses from Argon-Ion Laser at a Wavelength of 514.5 nm in the TEM_{00} Mode at a Pulse Repetition Rate of 10 Hz Lasting for 0.5 sec.

Eye No.	Energy/Pulse μJ
214	1.24
215	1.26
216	1.08
217	1.08
218	0.540
219	0.440
220	0.550
221	0.575
222	0.735
223	0.620
224	0.570
225	0.595
226	0.715
227	0.580
228	0.455
229	0.455
230	0.560
231	0.570
232	0.570
233	0.570
234	0.570
235	0.640
236	0.640
237	0.630
238	0.745
239	0.835
240	0.735
241	0.870
242	0.990
243	0.775

Table VIII. Retinal Burn Thresholds for Rhesus Monkeys' Eyes for Exposures to Trains of 10 μsec Pulses from Argon-Ion Laser at a Wavelength of 514.5 nm in the TEM_{00} Mode at a Pulse Repetition Rate of 100 Hz Lasting for 0.5 sec.

Eye No.	Energy/Pulse μJ
244	0.259
245	0.349
246	0.239
247	0.235
248	0.142
249	0.149
250	0.110
251	0.196
252	0.208
253	0.249
254	0.244
255	0.197
256	0.267
257	0.223
258	0.291
259	0.248
260	0.259
261	0.272
262	0.179
263	0.232
264	0.179
265	0.179
266	0.185
267	0.187
268	0.184
269	0.186
270	0.204
271	0.243
272	0.178
273	0.182

Table IX. Retinal Burn Thresholds for Rhesus Monkeys' Eyes for Exposures to Trains of 10 μsec Pulses from Argon-Ion Laser at a Wavelength of 514.5 nm in the TEM_{00} Mode at a Pulse Repetition Rate of 1 kHz Lasting for 0.5 sec.

Eye No.	Energy/Pulse μJ
274	0.182
275	0.159
276	0.176
277	0.174
278	0.138
279	0.149
280	0.186
281	0.163
282	0.186
283	0.154
284	0.127
285	0.151
286	0.131
287	0.082
288	0.123
289	0.128
290	0.158
291	0.103
292	0.167
293	0.190
294	0.208
295	0.116
296	0.115
297	0.150
298	0.137
299	0.176
300	0.154
301	0.156
302	0.152
303	0.190

Table X. Retinal Burn Thresholds for Rhesus Monkeys' Eyes for Exposures to Trains of 10 μsec Pulses from Argon-Ion Laser at a Wavelength of 514.5 nm in the TEM_{00} Mode at a Pulse Repetition Rate of 10 kHz Lasting for 0.5 sec.

Eye No.	Energy/Pulse μJ
304	0.130
305	0.106
306	0.144
307	0.117
308	0.105
309	0.082
310	0.102
311	0.086
312	0.068
313	0.082
314	0.122
315	0.136
316	0.134
317	0.100
318	0.065
319	0.062
320	0.078
321	0.067
322	0.150
323	0.151
324	0.114
325	0.139
326	0.144
327	0.144
328	0.161
329	0.157
330	0.151
331	0.116
332	0.113
333	0.114

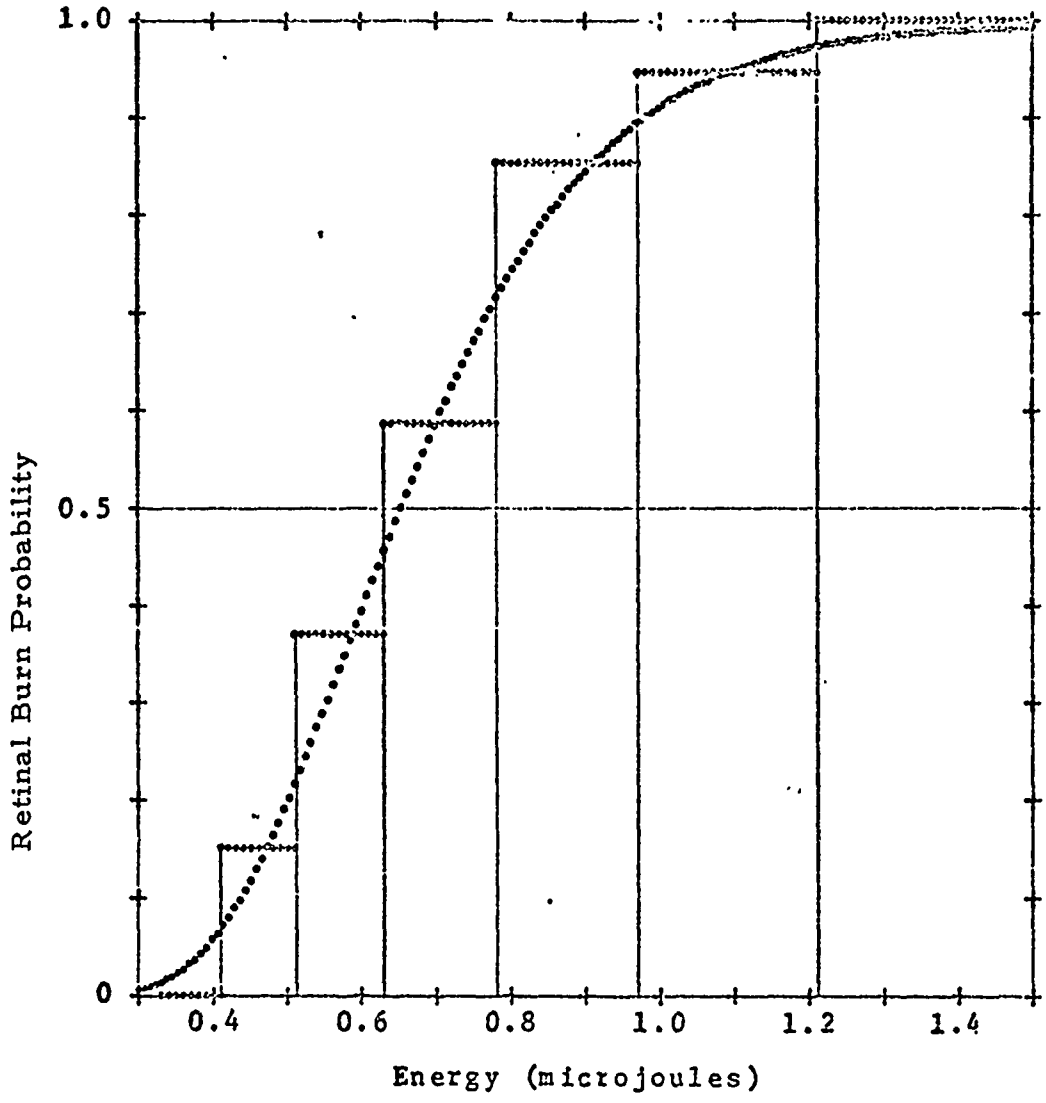

Figure 9. Retinal Burn Probability versus Energy per 10 μsec Pulse in the Pulse Train with a Pulse Repetition Rate of 10Hz. (30 eyes)

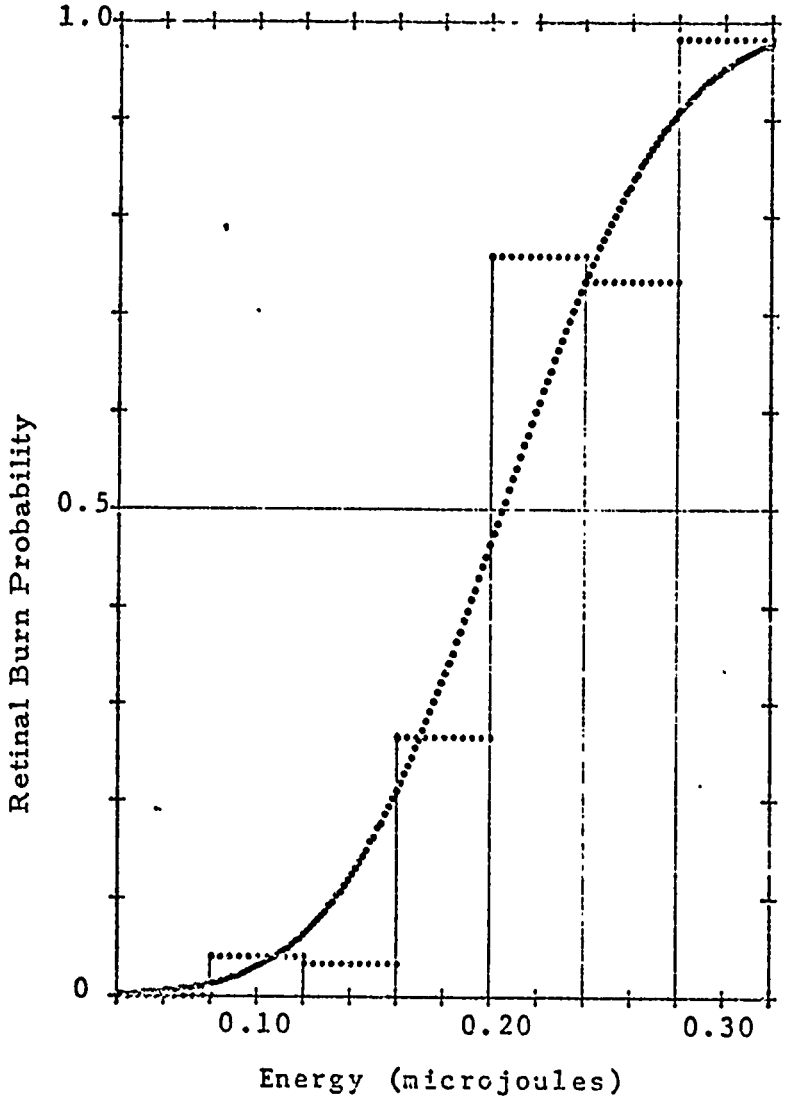

Figure 10. Retinal Burn Probability versus Energy per 10 μsec Pulse in the Pulse Train with a Pulse Repetition Rate of 1.00Hz. (30 eyes)

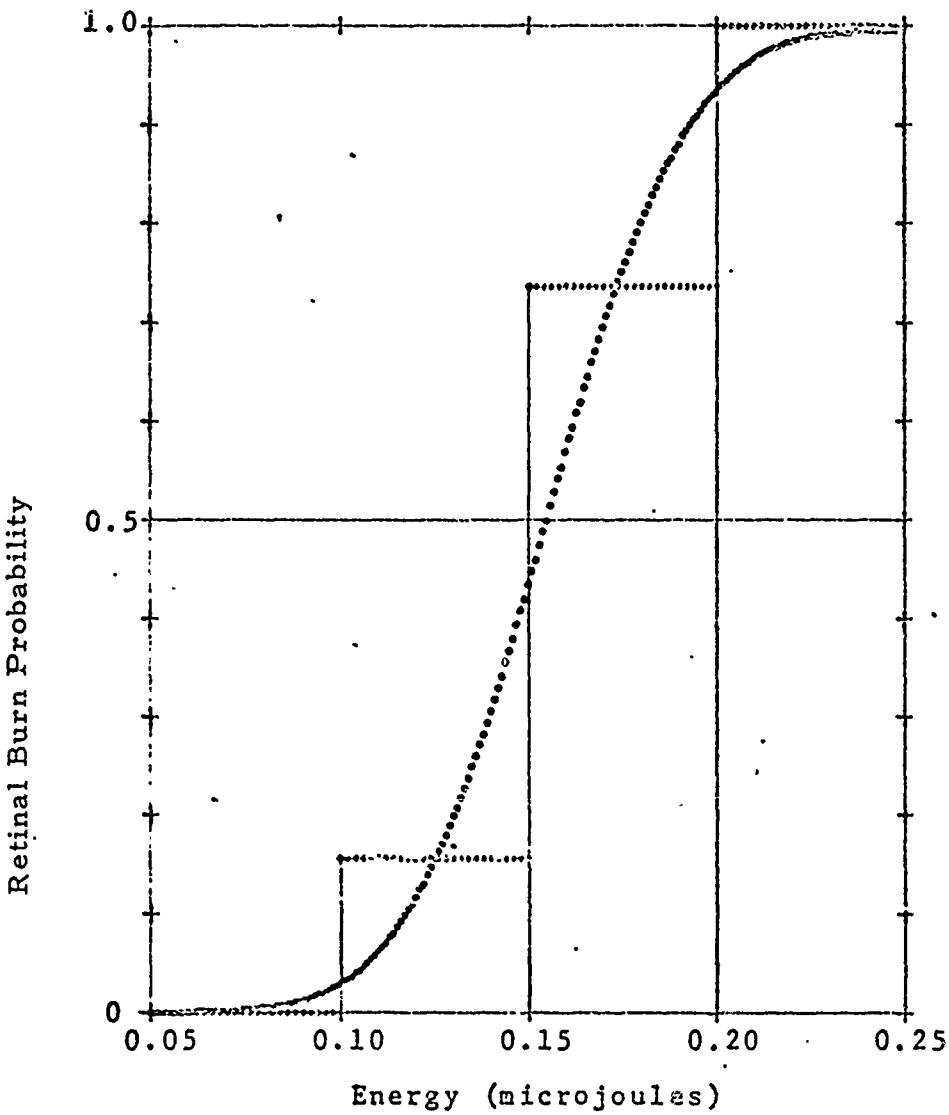

Figure 11. Retinal Burn Probability versus Energy per 10 μsec pulse in the Pulse Train with a Pulse Repetition Rate of 1kHz. (30 eyes)

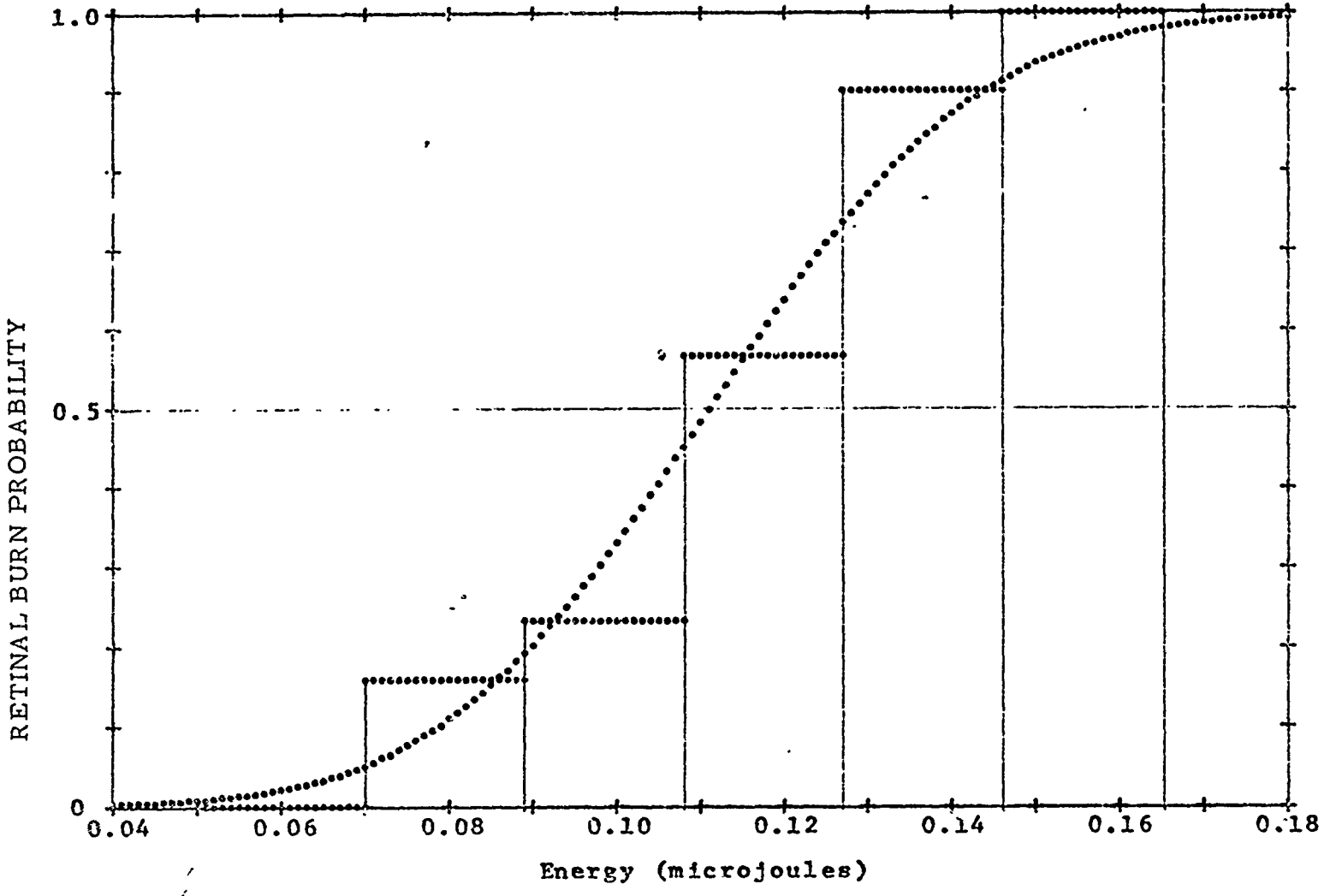

Figure 12. Retinal Burn Probability versus Energy per 10 μsec Pulse in the Pulse Train with a Pulse Repetition Rate of 10kHz. (30 eyes)

37

3.4 ED50 or P = 0.5 Energy-Values

Important quantities obtained in this study are retinal burn thresholds for the Macaca Mulatta exposed to single 10 μsec pulses and trains of the 10 μsec pulses of the 514.5 nm laser light. The retinal burn threshold (for the 1 hr criterion for the appearance of ophthalmoscopically visible lesions) is by definition the energy per pulse incident on the cornea which is expected to produce a retinal lesion in 50% of the Macaca Mulatta population having normal emmetropic eyes when this energy is focused into an exposed site in the macular region. These retinal burn thresholds are called the ED50 values or the retinal burn probabilities P = 0.5. The ED50 or the P=0.5 energy values can be obtained from either a probit analysis or from the mean of the retinal burn thresholds for a set of primate eyes. The ED50 or P=0.5 values obtained from these analyses for this study are shown in Table XI. These results and the other results described in this section will be discussed further in the following section of this report.

TABLE XI. Summary of ED50 or P = 0.5 Energy Values for Rhesus Monkeys' Eyes Exposed to Trains of 10μsec Pulses from Argon-Ion Laser at a Wavelength of 514.5 nm in the TEM_{00} Mode.

Repetition Rate Hz	Retinal Burn Threshold Energy/Pulse μJ								
	Probit			Arithmetical Mean			Logarithmic Mean		
	ED50	95% CL	σ	ED50	95% CL	σ	ED50	95% CL	σ
2 (Single Pulse)	1.6	0.1	0.3	2.0	0.3	0.8	1.80	0.06	0.18
10	0.65	0.04	0.14	0.71	0.08	0.2	0.68	0.04	0.12
100	0.21	0.01	0.06	0.22	0.02	0.05	0.21	0.04	0.10
1000	0.155	0.007	0.01	0.15	0.01	0.03	0.15	0.03	0.09
10000	0.111	0.009	0.02	0.12	0.01	0.03	0.11	0.04	0.12

σ refers to the standard deviation

95% CL refers to the 95% confidence level

4. ANALYSIS AND DISCUSSION OF RESULTS

Some remarks about the use of both (1) the probit analysis and the (2) the arithmetical average of the individual retinal burn thresholds to determine the ED50 value and/or the P=0.5 values are in order. An underlying assumption for using the probit technique to analyze these data is that the retinal burn/no burn observations are independent of any other retinal site and correspond to a random sample of the primate population. It appears that the retinal burn data like those compiled in Table I, for example, from observations on an eye may not be truly independent. To see why these retinal burn probabilities may arise from dependent observations consider the following: Measurements taken elsewhere [11] show that the sensitivity of the chorioretinal tissues to laser light varies by about a factor of 2 in going from the paramacular to the macular region and the latter is more sensitive than the former. Data for retinal burn thresholds taken for 30 primate eyes for a given exposure duration, e.g., data like those in Table II, reveal a variation of a factor of as much as 5 or 6 in the sensitivity of the macular region from primate to primate in the rhesus monkey population. If the factor of 5 or 6 is considered to be statistically valid, then the variability between eyes at random is larger than the variability within any particular eye [11]. Hence, it is possible that the frequency of observations used to determine retinal burn probabilities in any energy

interval is different than for the population[15]. If this is true, then the observations are not truly independent and the probit technique must be used with caution, if used at all. It is interesting to note that of the 5 sets of 30 primate eyes investigated in this study, only those listed in Table II and Table VII reveal retinal burn thresholds with spreads (ratio of highest to lowest values) that are only slightly greater than a factor of 2. It is interesting to note that the mean of the retinal burn thresholds for the 30 eyes in Table VII is 0.7 μJ with a standard deviation, σ, of 0.2 μJ. The two values in Table VII which cause the spread to be greater than the factor of 2 mentioned above have deviations from the mean value larger than 3σ. It is considered valid to discard values that differ from the mean by more than 3σ. If this procedure is followed with the data in Table VII, then the most probable value obtained for the retinal burn threshold is (0.6 ± 0.1) μJ and the remaining values left in Table VII have a spread of about 2. Following the same procedure with the values in Table II, the most probable value for the retinal burn threshold is (1.7 ± 0.6) μJ and the spread remaining is about a factor of 4. It is interesting to note of the five sets of primate eyes in this study and of the 6 sets of the previous study[6] at Technology Incorporated, only those values listed in Table II differ significantly by amounts greater than the factor of 2 from primate to primate. This tends to indicate there are still values in Table II with large systematic errors. If this is the case, then the conditions for use of the probit analysis may be satisfied, i.e. the variability between eyes of different primates are the same as the variation within a given primate eye in the rhesus monkey population.

It was the apparent difficulty[15] using the probit analysis that led to the determination of the ED50 values by computation of the arithmetical average for the set of 30 eyes irradiated by the laser for a given exposure duration. It is observed that the ED50 values obtained using the probit analysis and determined by the averaging technique agree well statistically. Moreover, it is noted that the 95% confidence limit intervals obtained are smaller for the probit analysis than for the averaging process. All reasons for the lack of agreement of the 95% confidence limit intervals using these two techniques is not known; but, it is suggestive of the fact that more observations are being used in the probit analysis than in the averaging process.

Some simple algebraic expressions involving the pulse width, τ, the pulse repetition rate, R, and the pulse train duration, T, are helpful to recognize and use in the analysis and discussion of the pulse train experiments. The number of pulses, n, that irradiate an eye in a single exposure by a pulse train is given by the product of R and T and is:

$$n = RT \tag{1}$$

It is obvious that the number of pulses, n, is on the interval

$$1 \leq n \leq T/\tau \tag{2}$$

The effective time, t, that an eye is irradiated during a single exposure by a pulse train is given by the product of n and τ and is:

$$t = n\tau \qquad (3)$$

These simple expressions will be referred to as needed in this analysis and discussion.

The data shown in Tables XI and XII reveal a cumulative effect of pulses in a repetitive pulse train. This cumulative effect implies that the subthreshold pulses, which have an energy below the threshold (based on the 1 hr criterion for the observation of ophthalmoscopically visible lesions) for a single pulse of the train, act in concert to cause a threshold (based on the same criterion) retinal burn for the pulse train.

In order to investigate this cumulative effect further, it is helpful to consider the threshold power per pulse in a pulse train in terms of the effective exposure time. These threshold powers per pulse from the probit analysis and the corresponding effective exposure times are shown in Table XII for the pulse trains used in these experiments. Note, the single pulse can be considered as belonging to the pulse train with a pulse repetition rate of 2 Hz and a duration of 0.5 sec, i.e., it is the lower limit on the pulse number for these trains shown in equation (1).

Table XII. A Summary of the Power per 10 μsec Pulse Corresponding to the Retinal Burn Probability of, P=0.5, for the Various Pulse Trains.

Pulse Train Number	Pulse Repetition Rate Pulses per sec	Effective Exposure Time (sec)	Retinal Burn Threshold Power mw/pulse
1	2	1×10^{-5}	157
2	10	5×10^{-5}	65
3	100	5×10^{-4}	21
4	1,000	5×10^{-3}	16
5	10,000	5×10^{-2}	11

With these results in mind, it would seem only natural to think that they are in accord with the predictions using a straightforward thermal model to describe the oculothermal processes involved--especially the thermal model [16,17] that treats properly the temporal effects of the laser energy deposition in, and the ensuing heat transfer by, the chorioretinal tissues involved. That these results would appear to be in accord with the predictions of a straightforward thermal model is shown by the data which reveal that the lower the pulse repetition rate the higher the power per pulse in the train to produce a threshold retinal lesion. This result should be expected in as much as, when the time between successive pulses in the train increases, more heat is transferred from the chorioretinal tissues involved allowing the temperature of these tissues to tend to the ambient value. When this model [16] is used to predict the effects of the repetitive pulse trains, it is found to give a result which agrees very well with that obtained in the single pulse exposure for a duration of 10 μsec. However, the predictions of the model disagree with the experimental results from the repetitive pulse trains. The cumulative effect is not predicted for these pulse trains for pulse repetition rates of about 100 Hz or less (except for the special 2 Hz case just mentioned). This prediction is in keeping with the prediction that the thermal relaxation time for the affected chorioretinal tissues involved is much less than the time interval

between pulses in these lower pulse repetition rate trains. This model predicts a cumulative effect for the trains involving pulse repetition rates of several hundred Hz or more but the net effect predicted is about an order of magnitude smaller than that which was measured in these experiments. The failure of the thermal model to predict accurately the cumulative effect for repetitive pulse trains is not understood. This failure could imply either one of two things or both. This failure could imply that the simple temperature criterion invoked is invalid under certain circumstances. In addition, this failure could imply that the oculothermal properties such as the optical absorption coefficient and the specific heat of the chorioretinal tissues involved are temperature and time-temperature dependent in these experiments. If the latter is the case, then it should be expected that the thermal model should fail to predict accurately the effects of long time duration, in excess of a few tens of milliseconds, single pulse exposures. Calculations have not been made with this model in this analysis to compare the results with data taken elsewhere [8, 11] for longer duration exposures using an argon-ion laser emitting a 514.5 nm beam in the TEM_{00} mode.

The idea that the data shown in Table XII indicate an accord with some thermal model, in concert with the revelation that the straightforward thermal model fails to predict all the cumulative effects observed,

suggests that these data be analyzed in an empirical manner. This empirical analysis could lead to a greater insight into the cause of the cumulative effect observed. In addition, this analysis may lead to an empirical model which could be a valuable guide as to which additional experiments need to be done employing repetitive pulse trains to enable laser safety experts to establish safe exposure levels without resorting to performing a very great number of oculothermal experiments, that would have to be done to completely scope the retinal burn threshold data needed to specify permissible exposure levels for Air Force personnel for all their laser systems. Moreover, such a model could reveal a criterion for threshold retinal lesion production which is more general and inclusive than the temperature criterion currently held in great respect at least for exposure durations in excess of about 10 μsec. Finally, the empirical model could form the basis for a theoretical model, which is more general than the thermal model, for the explanation of the complicated phenomena involved in the production of threshold retinal lesions with laser light. With these ideas in mind, an empirical analysis of the data was undertaken.

To begin this analysis, the logarithm of the threshold power per pulse was plotted versus the logarithm of the exposure time. This graph is shown in Figure 13. There are two curves in Figure 13. The solid

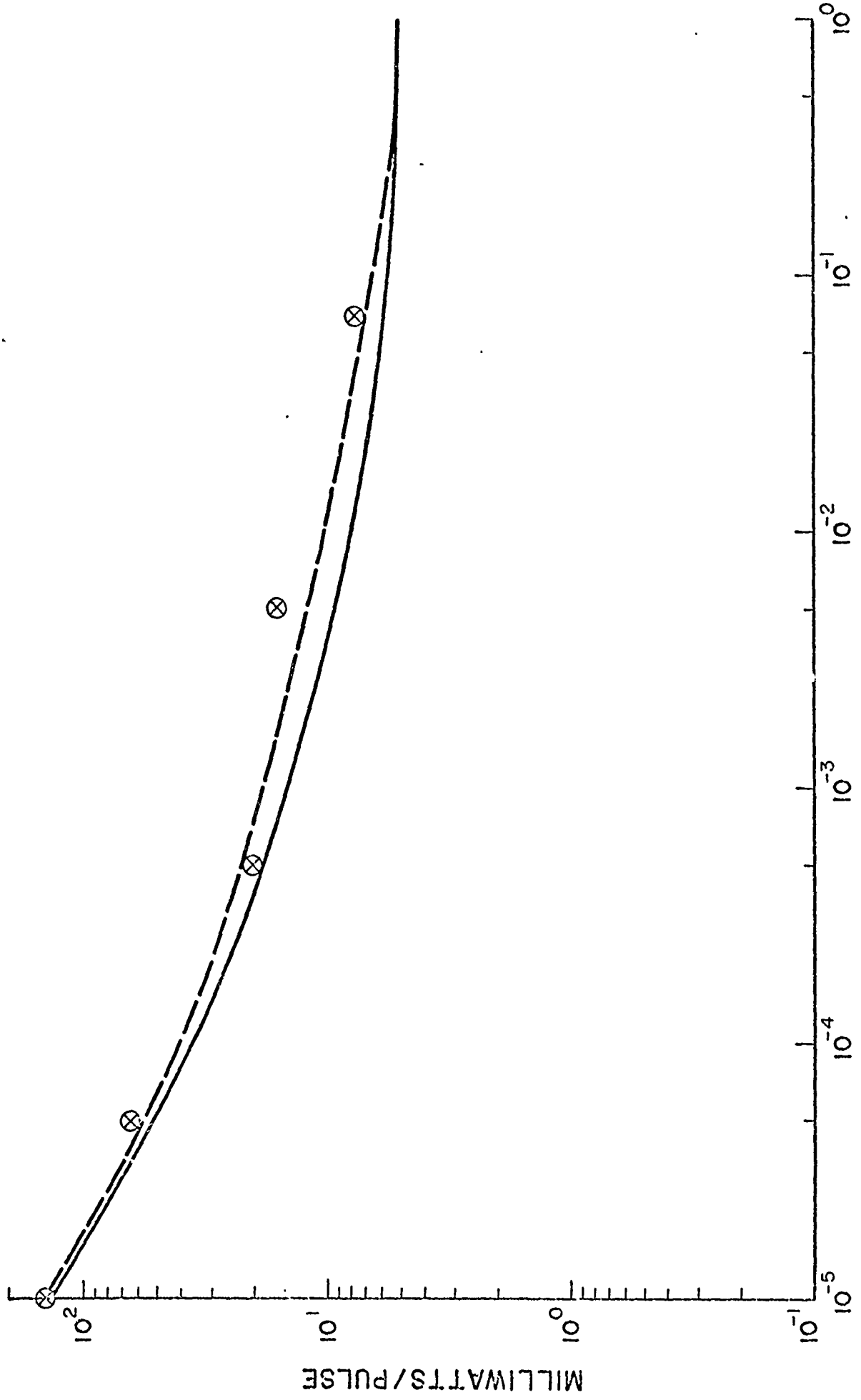

Figure 13. Power per Pulse at Threshold versus Time for Single Pulse (Solid Curve) and Repetitive Pulse Trains. (Dashed Curve).

curve is derived from single pulse irradiations of rhesus monkey eyes as a function of the exposure time. It must be pointed out that the solid curve is derived from data taken at two other laboratories [8, 11] and data taken at Technology Incorporated for argon-ion lasers with almost identical beam parameters--about the same divergence, the same wavelength and the beams in the TEM_{00} mode. To be complete, it must be pointed out further that there are no TEM_{00} mode data for argon-ion lasers for single pulse exposures with durations on the time interval from about 10^{-5} sec to approximately 2×10^{-3} sec. Consequently, the solid curve between 10^{-5} sec and 10^{-3} sec time intervals is a simple extension of the former [8, 11] long pulse exposures to the 10^{-5} sec exposure. The dashed curve represents a plot of the retinal burn thresholds, in terms of the power per pulse, versus the effective exposure times for the repetitive pulse trains. It is obvious why the two curves intersect at the 10^{-5} sec point since there is no known difference between a retinal exposure lasting for 10^{-5} sec and a retinal exposure from a train of 10 μsec pulses with a pulse repetition rate of 2 Hz lasting for 0.5 sec. Although we did not perform experiments on trains of 10 μsec pulses at a pulse repetition rate of 100 kHz lasting for 0.5 sec, it is clear, nevertheless, that the two curves should intersect at a time of 0.5 sec if the curves are composed of internally consistent data. That these data are internally consistent may be seen by the

following analysis.

Sliney summarizes data [4] indicating that a decrease by a factor of five in the amount of energy to cause a threshold retinal burn is to be expected for each order of magnitude decrease in the laser pulse width if the irradiated spot size is held uniform. Bresnick and coworkers [8] report results of experiments performed to determine retinal burn thresholds due to the long-pulse radiation of an argon-ion laser operating in the TEM_{00} mode at a wavelength of 514.5 nm. The beam divergence of Bresnick's laser was almost the same as ours and he analyzed the retinal burn data using the probit method. Bresnick and coworkers' results for the energy corresponding to the P=0.5 were extrapolated to the 10usec pulse regime. This extrapolation gave a value of approximately 1.6 μJ for the P=0.5 and is to be compared with 1.57 ± 0.07 μJ obtained in the probit analysis. This agreement is considered significant and is taken to imply that these two independent sets of data are internally consistent. That these two curves should intersect at 0.5 sec is obvious since the eye will note no known differences between an effective exposure time of $n\tau = \tau \times T/\tau$ and a single exposure of a duration T.

Several features of the solid and dashed curves in Figure 13 are noteworthy. First, there is insufficient experimental information to actually justify the manner in which the dashed curve approaches the

solid curve at the point of intersection at the 10^{-5} sec time value. This dashed curve is visually-fitted to the data from the repetitive pulse experiments. Since these experiments did not involve repetition rates between 2 Hz and 10 Hz, the shape of the dashed curve in the neighborhood of the 10^{-5} sec time value is not known. Certainly, one might expect that the train involving the 4 Hz repetition rate with 2 pulses separated by a time interval of 1/4 sec may be nearly equal power pulses implying that the dashed curve approaches this point of intersection in a direction nearly parallel to the abcissa. However, if this is the case, then it would appear that there would be a point of inflection on the dashed curve at this point of intersection. That the point of inflection is to be expected can be seen if one considers everything in a neighboring pulse train to be fixed with the exception that the pulse width is $\tau \pm \Delta\tau$ where $\Delta\tau$ approaches zero implying that this point of intersection moves tangentially to the solid curve. This observation implies that (1) the cumulative effect depends upon the pulse repetition rate, R, (2) the pulse train duration, T, and (3) the pulse width, τ. The fact that the cumulative effect depends on, R, and, T, is obvious when it is recognized that the dashed curve would have a different shape and a different endpoint for the upper limit of the effective exposure time. The fact that the dashed curve would have a different intersection for the lower limit (single pulse) of the effective exposure time implies that the cumulative effect is dependent upon the

pulse width, τ. The dependence of the cumulative effect upon the pulse width, τ, was verified by experiments using a neodymium-YAG laser performed at Technology Incorporated[6] as may be seen by the following discussion. The value for the threshold power per pulse for the train of 0.7 μ sec pulses at a pulse repetition rate of 1 kHz lasting for 0.5 sec is compared with the value obtained from the single 0.7 μ sec exposures. The former value is 2.1 watts whereas the latter value is 34.3 watts and these differ by a factor of about 17. Making a similar comparison for the results obtained for the power per pulse (15.7 mw) for the train of 10 μsec pulses at a pulse repetition rate of 1 kHz lasting for 0.5 sec with the value (157 mw) obtained for single 10 μsec exposures using an argon-ion laser, one finds that these two results differ by a factor of 10. These comparisons reveal that a cumulative effect exists for lasers operating in the repetitive pulse mode. This cumulative effect implies that pulses, subthreshold when taken separately, act in concert in the pulse trains to produce lesions in rhesus monkey eyes. Moreover, upon comparing the factor of 17 with the factor of 10, it is concluded that the size of the cumulative effect depends upon the FWHMP of the pulses composing the pulse trains. This conclusion is reached (1) because the pulse repetition rates (1 kHz) and the pulse train durations (0.5 sec) were the same for each laser and (2) because the results obtained for the retinal burn thresholds are based on enough

observations to make the experiments statistically valid.

A second noteworthy observation is made regarding contiguous points on the solid curve which taken together approximate a straight line segment. Pulse trains composed of pulse widths and duration times so as to cause the dashed curves to span this interval reveal thresholds on a power per pulse versus effective exposure times to be approximately the same as those on these straight line solid curve segments.

A third noteworthy observation regards the differences, as a function of time, between the solid and dashed curves for the pulse trains investigated. This difference reaches a maximum at about the mid-point of the duration of the pulse trains. Moreover, this difference is never greater than about 30%. This feature implies strongly that a few more experiments on trains of the same duration but composed of pulses about an order of magnitude and a half longer than the 10^{-5} sec used here would permit laser safety experts to, by extrapolation, establish accurately the permissible exposure levels for all repetitive pulse trains from argon-ion lasers of 0.5 sec duration and composed of pulses no shorter than 10^{-5} sec. A generalization of this observation is permissible. This generalization can be stated as follows. If it is expected that thermal phenomena are dominant in the lesion forming process, then it appears that a limited number of repetitive pulse experiments would enable laser safety experts to set accurately the permissible exposure levels for a

wide range of cases. These few experiments would involve the following. First complete the single pulse curve of power versus exposure time. Since thermal effects are believed to dominate the lesion forming process for exposures from 10^{-8} sec to a few seconds, the solid curve should be reasonably complete from exposures of a few seconds (say thru 30 sec) down to a few tens of nanoseconds, say about 2×10^{-8} sec. Secondly, the upper limit on the repetitive pulse effects for trains in this region would be spanned by pulse trains composed with pulses with width of about 2×10^{-8} sec with several pulse repetition rates and lasting for 30 seconds. The pulse width could then be taken at 10^{-7} sec, 10^{-6} sec, etc. to obtain about four additional intermediate curves. From these curves and by suitable interpolation between these curves, laser safety experts should be able to establish permissible exposure levels for all cases of interest, involving this laser, including single pulse exposures from 10^{-8} sec to 30 sec durations and all repetitive pulse trains in this time domain. This is indeed a great reduction of the very large number of experiments that might be considered possible for this purpose from the following discussion.

It is recognized that laser-ocular effects depend upon many parameters. These include, for the laser involved, the laser wavelength, beam divergence, temporal variation of the power (i.e., single pulse,

repetitive pulse), spiking nature of the pulses and the pulse duration time among others. From the oculothermal point of view, these parameters include: the size of the pupil, transmissivity of the intraocular media, the spectral absorption coefficient of the chorioretinal tissues, the heat transfer coefficient of the chorioretinal and contiguous tissues and the laser spot size at the retina among others.

Even when one recognizes that laser safety experts studying retinal effects arbitrarily divide the ocular effects into two categories, visible and near infrared, when wavelengths are considered, there are still many parameters which can be varied. Moreover, when it is recognized that these remaining parameters may themselves be functions of other parameters, e.g., time and temperature, the situation is still very complex indeed. A complete and detailed analysis of this problem would require highly sophisticated mathematical-computer techniques involving the solutions of complex functions involving numerous parameters. To consider solving such a problem appears to be a fantasy. Thus it makes sense to think of "worst-case" experiments, wherein most of the parameters are held fixed, for use in establishing permissible ocular exposure levels. This approach seems not only meaningful but necessary if lasers are to be used with any degree of assurance that they can be used with proper safeguards for the prevention of retinal damage.

Hence, it is seen that one can consider the worst case smallest spot size problems. Retinal burn probabilities can be determined under these conditions. These measurements can be used then to establish laser ocular safety criteria. Even with this approach, the overall problem is still very complex. However, it can be greatly simplified when it is recognized, for a given wavelength in conjunction with the worst case spot size, that the repetitive pulse experiments are tractable in terms of three parameters: the power at threshold, P, the pulse width, τ, and the pulse repetition rate, R. Thus, if one considers two wavelengths -visible and infrared -, the problem really begins to appear to be solvable.

However, even in this case, a solution to the problem could involve a great number of measurements, if the empirical approach suggested previously is not followed. To appreciate the fact that the situation is still very complex, consider the case shown in Figure 14 where the power at threshold is plotted versus τ and R. Such plots lead to surfaces in the P, τ, R three-space. If one wanted to, he could embark upon a program to map out these surfaces in the P, τ, R three space. If such an approach were considered, its complexity can be revealed by a few plots projected onto the P, R and P, τ planes as various parameters are varied as shown in Figure 15. An easier way out would probably be just to take every laser that Air Force personnel

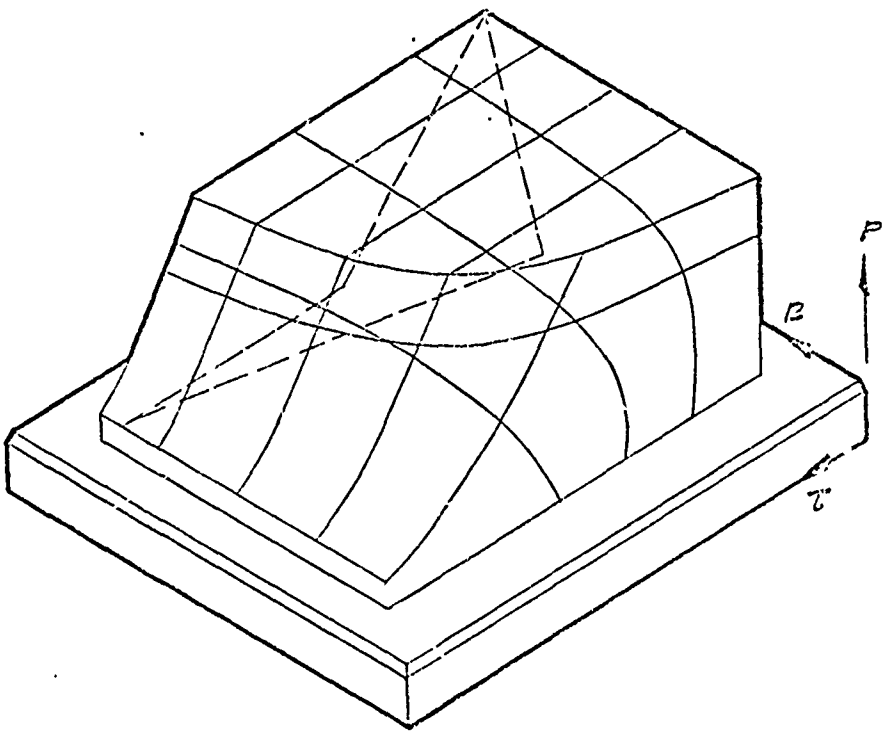

Figure 14. Relationship Between Threshold Power, (P), Pulse Width (τ) and Pulse Repetition Rate (R) for Laser at Given Wavelength in TEM_{00} Mode.

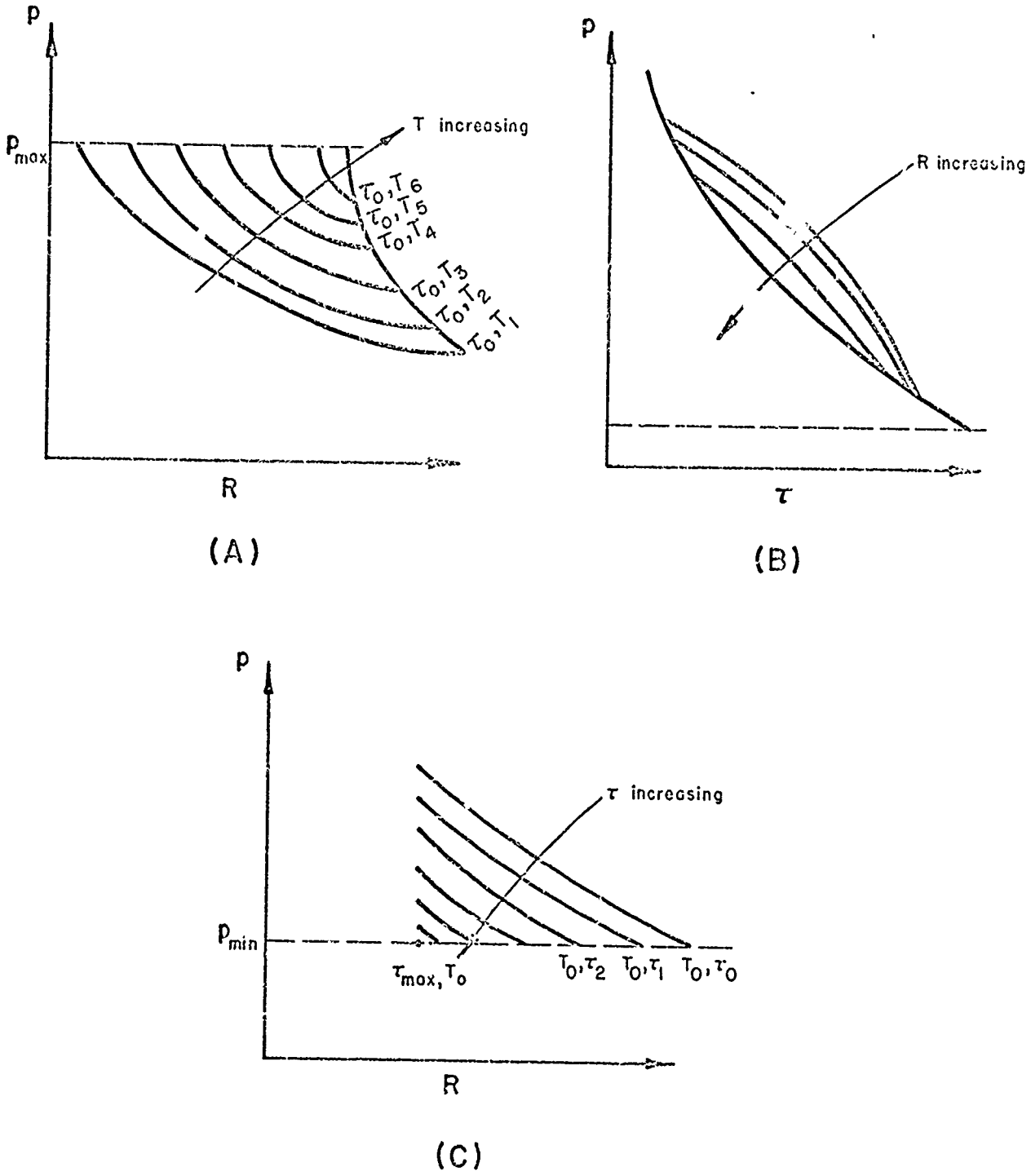

Figure 5. Projections of Threshold Burn Surfaces in p, τ, R Three-Space onto Corresponding Two-Dimensional Planes.

acquire and use it to perform retinal burn probabilities and establish ocular effects safety criteria for this laser; but, this approach could lead to serious delays in testing and fielding laser devices.

A more meaningful and less costly approach would appear than outlined previously. This involves a minimum of pulse train exposures involving a laser emitting radiation in the visible region (say argon-ion) and one in the near-infrared (say Nd^{3+}-YAG).

One possible goal in addition to producing the threshold power versus pulse duration and effective pulse exposure time could be to establish a threshold for repetitive pulses in general. This would be to find, for a given subthreshold power pulse, the time interval between pulses such that no retinal lesion would occur regardless of the duration of the pulse train. This appears to be of more than academic interest because of the long term destructive light adaptation[17] effects that may occur. Even though one experiment was performed[18] that might shed some light on the nature of this pulse train threshold it likewise suggests some problems involved and alternate explanations of the results obtained[18]. First one must clearly show the waveform of the laser light used. If long pulse laser systems are used and the pulses obtained by pumping by pulsed flashlamps, it may contain spikes. These spikes can be about 0.1 to 2 μsec wide and occur at a rate of a few to many MHz. Moreover, the power in individual spikes may exceed

the average power of the pulse by as much as a factor of five. Consequently, the effect observed under such circumstances would be very difficult to interpret. This fact can be appreciated very well when it is recognized that the spiking corresponds to transverse "mode-hopping" and the high power peaks may correspond to the TEM_{00} mode and correspondingly low beam divergence and smallest retinal spot size. Secondly, one must be careful to keep the observation times of the retinal burn thresholds the same in experiments like these. If the one-hour criterion is used for the single pulse exposure, then this must be used for the repetitive pulse exposures. It is not clear that this was done in the repetitive pulse exposures with 1 to 3 min. intervals between pulses reported[18]. It is entirely possible that a subthreshold exposure can cause a lesion if the observation time is inadvertently increased from 1 hour to say 2 to 5 hours.

Finally, it is observed, from Figure 13, that there is a dearth of experimental data available for lasers operating at visible wavelengths in the TEM_{00} mode. For these conditions, there are no retinal burn threshold data for (1) single pulses shorter than 10^{-5} sec, (2) single pulses having durations from 10^{-5} sec to 10^{-3} sec, (3) single pulses having durations longer than 1 sec and (4) repetitive pulse trains other than the one reported in this work.

5. SUMMARY AND CONCLUSIONS

An argon-ion laser was operated at a wavelength of 514.5 nm in the TEM_{00} mode. The output beam of this laser was modulated to produce single 10usec pulses and trains of 10u sec pulses. The pulse repetition rate was varied from train to train and was, in turn, 10 Hz, 100 Hz, 1 kHz and 10 kHz. The duration of every pulse train was 0.5 sec. Eyes of rhesus monkeys were irradiated with the single 10usec pulses and by these pulse trains; and, a retinal burn threshold was determined for 30 primate eyes for each case. The data obtained were analyzed using a probit technique. From this probit analysis, the energy for a single 10usec pulse and the energy per pulse in a train corresponding to the retinal burn probability of P = 0.5, i.e. the ED50 value, was determined for pulse trains corresponding to the different pulse repetition rates. The ED50 values found were (1.6 ± 0.1) uJ, (0.65 ± 0.03) uJ, (0.21 ± 0.01) uJ, (0.157 ± 0.006) uJ and (0.11 ± 0.009) uJ, a confidence level of 95% for the single pulse and for the 10 Hz, 100 Hz, 1 kHz and 10 kHz pulse trains, respectively. The corresponding results obtained with the arithmetical averaging method were (2.0 ± 0.3) uJ, (0.71 ± 0.05) uJ, (0.22 ± 0.02) uJ, (0.15 ± 0.01) uJ, and (0.12 ± 0.01) uJ. Each of these energies was less than ED50 value of 1.57 ± 0.14 uJ, at a confidence level of 95%, and (1.96 ± 0.30) uJ, respectively, using the probit and averaging techniques on single 10 usec pulse retinal burn threshold data from the same laser. Hence a cumulative effect was discovered for pulses in the repetitive pulse trains; and, this result is in agreement

with the result found using a Nd^{3+}-YAG laser operated in the repetitive pulse mode [4]. In the context used herein, the term cumulative effect means that subthreshold pulses based on the 1 hr criterion act in concert to produce retinal lesions. The cumulative effect observed with the pulse trains from the argon-ion laser in conjunction with that observed using the Nd^{3+}-YAG laser indicates that this effect is dependent upon the width of the pulses composing these trains and the pulse repetition frequency. Moreover, a subsequent empirical analysis revealed that the cumulative effect is dependent upon the pulse train duration.

The exact nature of the cumulative effect is not understood. It was found that, by using a straightforward thermal model based on a temperature criterion for lesion production, one was unable to predict the cumulative effect observed experimentally. This failure, by using the thermal model, to predict the cumulative effect led to the interpretation of the experimental results using empirical considerations. In this empirical analysis, the logarithm of the power per pulse at the retinal burn probability, P = 0.5, was plotted versus the logarithm of the effective exposure time for each pulse train. This plot was performed on the same graph as that used to plot the results of the corresponding experiments using single pulse exposures. The empirical analysis showed that these two curves intersected at

the time corresponding to the duration of a single pulse, 10 μsec, and at the time corresponding to the duration of a train, 0.5 sec. Moreover, this analysis revealed that these two curves differed at most by 30% and that this difference reached a maximum at about the midpoint of the pulse train durations.

This result indicated that, based on the results of a relatively few well chosen repetitive pulse laser experiments, laser safety experts could establish permissible exposure levels for a wide range of laser systems, not only for single pulse exposures but also for exposures to repetitive pulse trains. The term relatively few here has an obvious meaning when one considers the alternate possibilities: (1) individual determination of the retinal burn threshold for every new laser system and (2) performing the very large number of experiments required to map out the retinal burn thresholds in the P, τ, R three space.

6. REFERENCES

1. R. G. Allen, et al. "Research on Ocular Effects Produced by Thermal Radiation", Final Report, USAF Contract No. AF41(609)-3099, July 1967.
2. R. G. King and W. J. Geeraets. "The Effect of Q-Switched Ruby Laser on Retinal Pigment Epithelium in Vitro", Acta Ophthal. 46, 617 (1968).
3. A. M. Clarke. "Ocular Hazards" (Handbook of Lasers with Selected Data on Optical Technology, Robert J. Pressley, Ed.) Chemical Rubber Co., Cleveland, Ohio, 1971, Page 3-10.
4. D. H. Sliney. "The Development of Laser Safety Criteria-Biological Considerations" (Laser Applications in Medicine and Biology, Volume I, M. L. Wolbarsht, Ed.), Plenum Press, New York 1971, Page 163-238.
5. A. Vassiliadis. "Ocular Damage from Laser Radiation" (Laser Applications in Medicine and Biology, Volume I, M. L. Wolbarsht, Ed.), Plenum Press, New York 1971, Page 125-162.
6. C. H. Skeen, W. Robert Bruce, J. H. Tips, Jr., M. G. Smith and G. G. Garza. "Ocular Effects of Near Infrared Laser Radiation for Safety Criteria", Contract No. F41609-71-C-0016, Draft Final Report, April 1972.
7. Irving L. Dunsky and Paul W. Lappin "Evaluation of Retinal Thresholds for C. W. Laser Radiation" Vision Res. 11, 733 (1971).

8. G. H. Bresnick, et al. "Ocular Effects of Argon Laser Radiation", Investigative Ophthalmology 9, 901 (1970).

9. William T. Ham, Jr., Walter J. Geeraets, Harold A. Mueller, Ray C. Williams, Alexander U. Clarke and Stephen F. Cleary. "Helium-Neon Laser in the Rhesus Monkey", Arch. Ophthal. 84, 798 (1970).

10. George D. Frisch, Edwin S. Beatrice and Robert C. Holsen. "Comparative Study of Argon and Ruby Retinal Damage Thresholds", Investigative Ophthalmology 10, 911 (1971).

11. A. Vassiliadis, R. C. Rosan and H. C. Zweng. "Research on Ocular Laser Thresholds", Final Report Contract F41609-68-C-0041, August 1969.

12. G. Wald and D. R. Griffin. "Change in Refractive Power of Human Eye in Dim and Bright Light", J. Opt. Soc. Am., 37, 321 (1947).

13. R. E. Bedford and G. Wyszecki. "Axial Chromatic Aberration of the Human Eye", J. Opt. Soc. Am., 47, 564 (1957).

14. D. J. Finney. Probit Analysis, Second Edition, Cambridge University Press, New York, New York, 1952.

15. Richard McNee. A Private Communication.

16. M. Mainster, T. J. White, J. H. Tips and P. W. Wilson. "Retinal Temperature Increases Produced by Intense Light Sources" J. Opt. Soc. Am., 60, 264 (1970).

17. M. Mainster. "Destructive Light Adaptation" Ann. Opthal., 2, 44 (1970).

18. Gordon L. M. Gibson. "Retinal Damage from Repeated Subthreshold Exposures Using a Ruby Laser Photocoagulator", SAM-TR-70-59, October 1970.

19. A. Goldstein. "Biostatistics", MacMillian Co., New York, 1964, Page 177.

APPENDIX A
ARGON-ION LASER SYSTEM

The laser used in this program is the Coherent Radiation Incorporated model 52G-A argon-ion laser. A schematic diagram of the cavity of this laser system is shown in Figure 16. Without either the prism-wavelength-selector or the acousto-optical shutter in the laser cavity, this laser emits a total cw power of 3.0 W for all lines in the TEM_{00} mode. The beam diameter was 1.5 mm at the $1/e^2$ points in its radial energy distribution.

Acousto-Optical Shutter

To obtain 10 μsec pulses and trains of these pulses, a modulator was inserted into the laser cavity. This modulator was the Coherent Radiation Incorporated model 462 acousto-optical shutter. With this modulator inserted into the cavity and before its activation, the cw output power of the laser was reduced to 2.78 W. When the quartz crystal of this shutter was activated by a 25 MHz R-F electromagnetic field, the output power of the laser was modulated. This modulation was produced by the increase in the diffraction losses of the laser cavity when the R-F was applied to the crystal. These diffraction losses occurred in accordance with the Raman-Nath effect. The crystal behaved as a diffraction grating when the R-F was applied

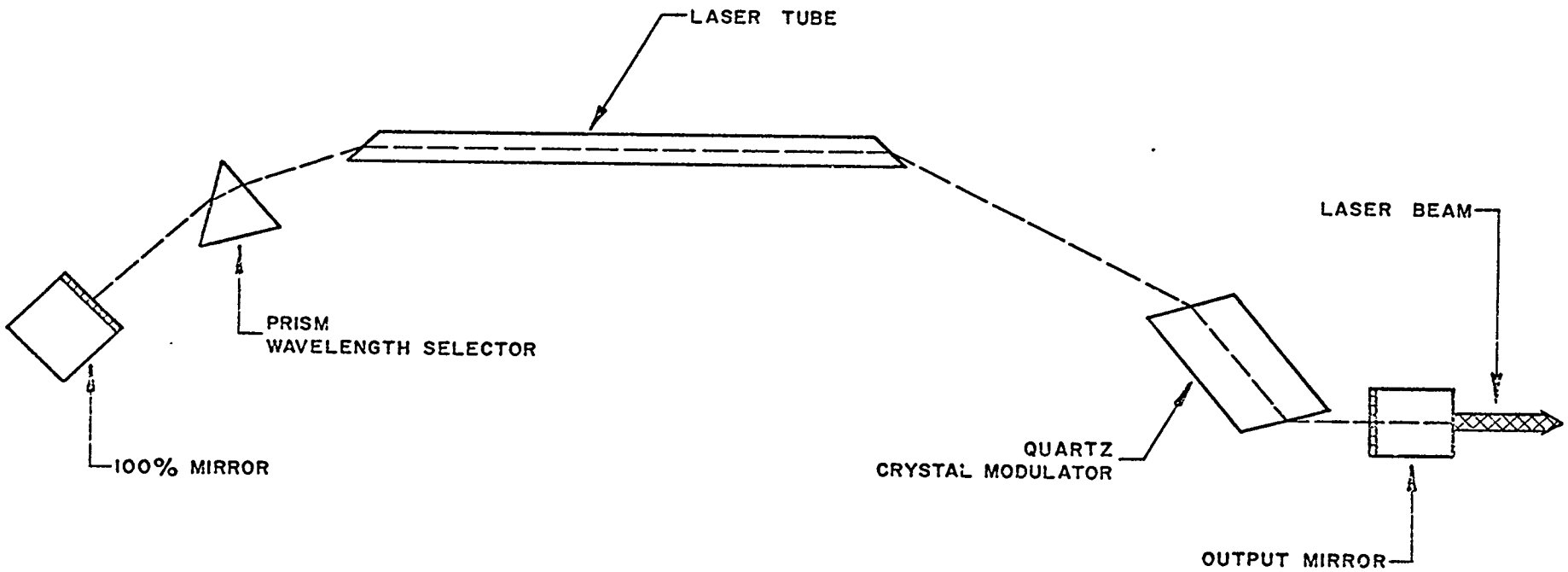

Figure 16. A Schematic Diagram of the Argon-Ion Laser Cavity

and the diffraction losses of the cavity became so large laser activity cannot occur. If the R-F was gated-off the crystal suddenly, the cavity gain returned very suddenly to its quiescent value and laser activity ensued instantaneously. This laser activity continued until the R-F signal was applied to the crystal again.

The R-F field on the crystal was varied by an electrical control box which was an integral part of the laser system. This control system permits the selection of single pulses of durations which were continuously variable from 2 μsec to cw. Moreover, trains of these pulses could be selected with pulse repetition frequencies which were continuously variable from 0.5 Hz to 50 kHz, provided the pulse widths and their duty cycle were not mutually exclusive.

The acousto-optical shutter was a Q-switch in the sense that it controls the Q-value of the laser activity. However, it was not a Q-switch in the sense that energy is stored in the cavity and released suddenly with a large peak power enhancement. The modulation was performed so that the peak power of the pulses was constant and equal to the cw power corresponding to the same argon-ion gas discharge tube load-line condition in the absence of the shutter.

Prism Wavelength Selector

With the shutter placed in the cavity and the R-F power controlled to

to obtain 10 μsec pulses, it was found that a modulation occurred. However, the laser beam was not fully modulated since the 10 μsec pulses occurred in the presence of a large background of cw radiation. This cw background radiation occurs at 488 nm. The cw background arises because the gain of the laser cavity at this line, in concert with the population inversion, is too large to be overcome by the Raman-Nath effect induced diffraction losses.

For the purposes of this program, this cw background radiation would be untenable because single "clean" pulses and trains of these "clean" pulses were needed to meet the requirements of this experimental program.

To obtain the pulses required, a prism wavelength selector (Coherent Radiation Inc., model 431) was inserted into the cavity as shown in Figure 16. By proper orientation of the prism, the various laser lines in the argon-ion gaseous electronic discharge are selected in turn for emission - the others being refracted from the cavity. With this prism wavelength selector, the laser emission power was measured at the various lines and the results obtained were as displayed in Table XIII.

Table XIII. Laser Power versus Wavelength using the Prism Wavelength Selector

Line nm	Power Watts
514.5	1.30
501.7	.225
496.5	.435
488.0	1.05
476.5	.465
472.7	.130
465.8	.075
457.9	.230

It is pointed out here, for emphasis, that the blue line at 488 nm could not be fully modulated - all remaining lines were fully modulated. The data listed in Table I indicates the green line at 514.5 nm yielded a power of 1.3 watts cw in the TEM_{00} mode. Since this line has a greater power than any of the other fully modulated lines, it was chosen as the wavelength to perform the experiments for this program.

APPENDIX B
LASER SYSTEM CALIBRATIONS

Procedures were established for laser calibrations for determining the instantaneous pulse power, shape and energy. The configuration of the experimental arrangement used in the laser system calibrations was that shown schematically in Figure 17. This same arrangement was used in the retinal irradiations except in the latter primate eyes, in turn, replaced the ballistic thermopile and/or the power meter. The similarity between the calibration and retinal irradiation arrangements is mentioned here because the radial energy distribution in the laser beam was purely TEM_{00} until it impinged upon the beam splitter, the "pop-up" mirror and various detectors. The arrangement for these measurements induced noise into the TEM_{00} mode. This noise was completely suppressed by placing an iris diaphragm to the left of the beam splitter in Figure 17 and using the proper aperture in the iris. The noise suppression procedure was used during all of the calibrations and the retinal irradiations. Hence, all irradiations were performed using 514.5 nm radiation in the pure TEM_{00} mode.

Laser Pulse Waveform

The laser pulse waveform was determined using a SGD-100 diffuse silicon photodiode. For our experiments, the sensitive face of this detector was covered with a thin plate of alumina. This Al_2O_3 plate

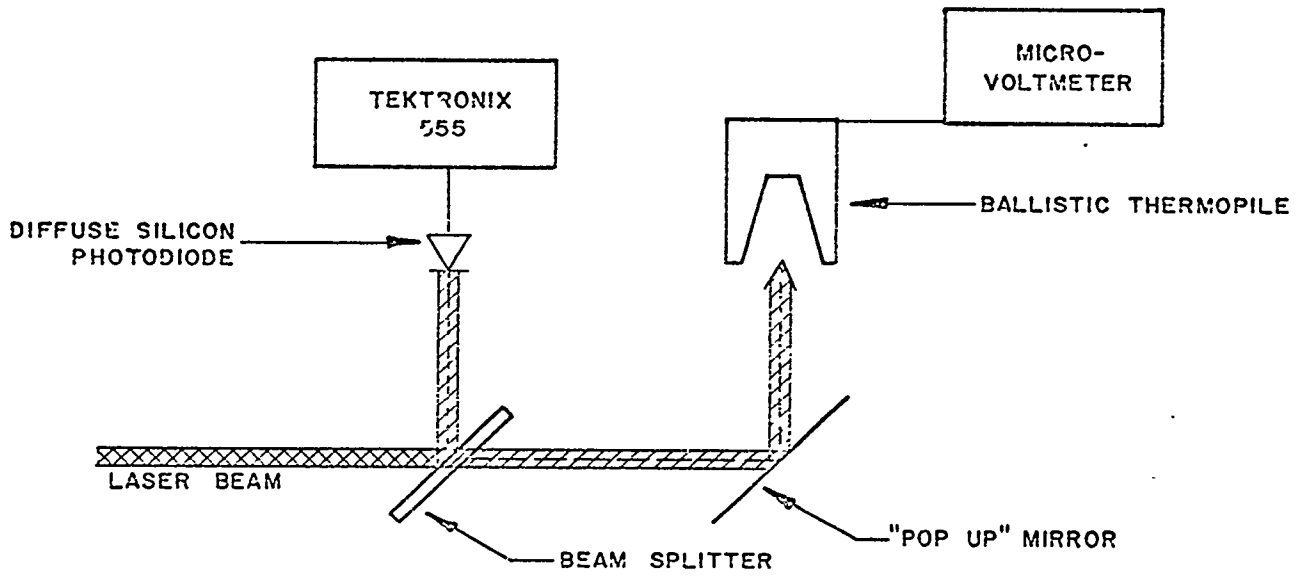

Figure 17. A Diagram of the Laser Calibration Arrangement

served both to attenuate the laser beam incident thereon and to make the irradiation thereof more complete and uniform.

The output of this photodiode was measured using a Tektronix model 555 dual beam oscilloscope. By using the proper neutral density filters, it was shown that the SGD-100 photodiode, with a reverse bias of 30 volts, responded linearly when detecting the 10 μsec pulses and the full cw power of the 514.5 nm line. With this arrangement, the waveform for every retinal irradiation was detected and shown to be 10 μsec at the half-maximum-power points.

Laser Pulse Energy

Great care was taken in calibrating the laser and detector system to determine the energy of the 10 μsec pulses. Extreme care was exercised because this energy is one of the basic parameters used in defining the retinal burn threshold.

A key factor in the calibration procedure was the concept that the acousto-optical shutter does not vary the peak power of the laser output from the value obtained when this modulator was in its quiescent state. It was important to realize that this peak power remained constant because of the manner, discussed later, in which the SGD-100 photodiode was calibrated and used to detect both the laser pulse waveform and the laser pulse energy. Moreover,

it was deemed necessary to calibrate the photodiode relative to two independent detectors with traceability to the National Bureau of Standards. The two absolute detectors available for this purpose were a HADRON/TRG model 100 ballistic thermopile and a Coherent Radiation Incorporated model 201 power meter. The ballistic thermopile is inherently a detector for pulsed energy sources and the power meter is a detector for cw power sources.

The ballistic thermopile was not sensitive enough to measure the energy in the 10 μsec pulses. It had a sensitivity of 198 μv/J and was calibrated to give reliable responses only as small as 0.3 μv provided the energy was delivered in 5 sec or less. Thus the lower limit of the pulse energy it could measure reliably was 1.5 mJ. The 10 μsec pulses contained a maximum of about 13 μJ. This pulse energy was clearly beyond the range for reliable detection by the ballistic thermopile. The power meter will not handle the pulsed operation in any case. With these ideas in mind the SGD-100 photodiode calibration procedure was as follows:

The photodiode was arranged to be responding, to the 514.5 nm light, in its linear range as described previously. The waveform of the 10 μsec pulses was then recorded by the dual beam oscilloscope. The R-F power was then gated-off the quartz crystal while simultaneously being careful to maintain the same peak power in the cw mode as recorded in the

1 μsec pulses. This corresponding cw beam was detected then by the model 201 power meter and the power, P, was recorded in watts. Thus the energy of the pulses, W_P, in joules is

$$W_P = 10 \times 10^{-6} (\text{sec}) \times P \qquad (1)$$

This procedure gave one absolute calibration of the responses of the photodiode to the 10 μsec pulses as recorded by the dual beam oscilloscope.

As independent absolute calibration was obtained using the ballistic thermopile. Maintaining the peak power the same as that for the 10 μsec pulses and the cw power mentioned previously, the R-F function switch was arranged so the laser emitted a pulse of the 514.5 nm light which was short compared to the 5 sec time constant of the ballistic thermopile but which had sufficient energy to be detected reliably thereby. For the calibrations for this study, this pulse width was about 132 msec. The corresponding pulse energy, W_{TP} in microvolts was detected with the ballistic thermopile in conjunction with a Kiethley model 150 B microvoltmeter. The energy, W_P in joules, for the 10 μsec pulses from these measurements is:

$$W_P = [W_{TP}/198] \times \frac{10 \times 10^{-6} \text{ sec}}{132 \times 10^{-3} \text{ sec}} \qquad (2)$$

It is interesting to note that the ballistic thermopile and the power meter measure their respective laser parameters with an accuracy of ± 5%; and, the two independent calibrations agreed to within the corresponding expected statistical deviations. These two independent and absolute methods for calibrating the SGD-100 photodiode for detecting the energy per 10 μsec pulse were followed each day the retinal irradiations were performed.

APPENDIX C

Statistical Analyses of Data

One analysis is performed according to the method described by Finney[14] except that the weighting coefficients and working probits are calculated from formulas instead of being selected from tables. All calculations are performed automatically by a Wang 700 programmable calculator. The graphical plot of the data is generated automatically from the resulting parameters by means of a Wang 702 plotting output writer operating in conjunction with the calculator.

The data for a typical probit analysis consist of a set of energy bands $\{[e_i, e_{i+1}]\}$ together with the number of burns, n_i, and the number of trials, N_i, in each band. The lowest energy band $[e_0, e_1]$ used in the analysis is usually the highest for which there are no burns at energies below e_1. The highest band used $[e_M, e_{M+1}]$ is normally the lowest for which there are 100% burns at energies above e_M. Each energy band is actually represented for analysis purposes by the energy at the midpoint: $E_i = \frac{1}{2}(e_i + e_{i+1})$ for $i = 0, 1, 2, \ldots, M$.

Probit analysis begins with the assumption that the burn probabilities. $p_i = n_i/N_i$, are approximately normally distributed with respect to either the energies or the logarithms of the energies. The logarithms are generally to be preferred since they have the doubly infinite range $(-\infty, \infty)$

which is the proper domain of the normal (gaussian) distribution function. For an appropriately restricted domain, however, the energies themselves may provide a distribution of probabilities more nearly normal, according to the chi-square statistic, than for their logarithms; in which case the choice is problematical. In either case the domain is represented in the analysis by x_i (=logE_i or E_i) for i = 0, 1, 2, ..., M.

The normal distribution of x, with mean μ and standard deviation σ, is given by

$$P_i = P\{x \le x_i\} = \frac{1}{\sqrt{2\pi}} \int_{-\infty}^{(x_i-\mu)/\sigma} e^{-y^2/2}\, dy$$

(distribution function)

The upper limit of integration is called a probit. A probit is customarily defined as 5 more than $(x-\mu)/\sigma$, which is called a normal equivalent deviate (NED). Probits thus simplify hand calculations by being positive in all but 3 cases out of ten million. Positive probits are neither necessary, practical, nor desirable for automatic machine computation. Therefore, in this paper probit = NED. This probit is seen to be a linear function of x. Therefore, the probit Y_i corresponding to x_i is

$$Y_i = \alpha + \beta x_i$$

where $\alpha = -\mu/\sigma$ and $\beta = 1/\sigma$. The parameters α and β are initially estimated and then improved by iteration of the following algorithm:

1. Calculate Y_i and P_i;
2. Adjust Y_i to a value y_i corresponding to p_i;
3. Apply weighted linear regression analysis to $y_i = \alpha + \beta x_i$ to find new values for α and β.

Adjustment of the probits is accomplished by making use of the facts that

$$\frac{dP}{dy} = Z(y) = \frac{1}{\sqrt{2\pi}} e^{-\frac{1}{2}y^2} \quad \text{(density function)}$$

and

$$\frac{p_i - P_i}{y_i - Y_i} = \frac{\Delta P}{\Delta Y} \doteq \frac{dP_i}{dy} = Z(Y_i) = Z_i.$$

Therefore, $y_i = Y_i + (p_i - P_i)/Z_i$ is the appropriate adjustment.

Weights to be appended at each point, (x_i, y_i), for the regression analysis have been derived by means of the maximum liklihood method[14]. Combining these with the "natural" weights, i.e. the number of trials in each of the associated energy bands, yields the effective weights

$$w_i = \frac{N_i Z_i^2}{P_i(1-P_i)}$$

The parameters α and β are calculated as the solution of the normal equations

$$\alpha \Sigma w + \beta \Sigma wx = \Sigma wy$$

$$\alpha \Sigma wx + \beta \Sigma wx^2 = \Sigma wxy$$

where all summations are over i, i = 0, 1, 2, ... M, and subscripts are implied by the sigmas. The solution is

$$\beta = \frac{\Sigma w \Sigma wxy - \Sigma wx \Sigma wy}{\Sigma w \Sigma wx^2 - (\Sigma wx)^2}$$

$$\alpha = \frac{\Sigma wy}{\Sigma w} - \beta \frac{\Sigma wx}{\Sigma w} = \bar{y} - \beta \bar{x}.$$

The sequences $\{\alpha_k\}$ and $\{\beta_k\}$, produced by repetition of the foregoing algorithm, are not conveniently useful for deciding when to terminate the iterations. The sequence of functions $\{f_k : f_k(x) = \alpha_k + \beta_k x\}$ can, however, be used easily for testing the goodness of fit of the n_i to their expected values by means of the chi-square statistic. Since $Y_i = f_k(x_i)$, for any particular k, and $P_i = P(Y_i)$, the expected value of n_i is $N_i P_i$. Chi-square is calculated[19] by

$$\chi^2 = \sum_{i=0}^{M} \frac{(N_i P_i - n_i)^2}{N_i P_i (1 - P_i)}$$

and the algorithm is terminated when this quantity is stabilized to three decimal places.

The mean value of x is that value, μ, for which $y = \alpha + \beta\mu = 0$, or $\mu = -\alpha/\beta$. The median effective energy (dose) for producing a burn is

$$ED50 = \begin{cases} \mu & \text{if } x = E \\ 10^{\mu} & \text{if } x = \log E \end{cases}$$

and the 95% confidence limits are obtained from

$$\mu + \frac{(\mu - \bar{x})G}{1 - G} \pm \frac{1.96}{\beta(1-G)} \sqrt{\frac{1 - G}{\Sigma w} + \frac{(\mu - \bar{x})^2}{\Delta}},$$

where $$G = (1.96)^2/(\beta^2\Delta)$$

and $$\Delta = \Sigma wx^2 - (\Sigma wx)^2/\Sigma w,$$

the conversion for $x = \log E$ being obvious.

Three distribution functions were tested in place of the gaussian both to verify the results of the analysis and to determine a possible preference for one of these alternative distributions. The three functions and their associated densities are given in Table XIV.

In only two of eight cases for which the tests were made did the gaussian fit the data best according to the chi-square statistic. The logistic distribution had the smallest χ^2 in half the cases and the arctangent distribution led in the remaining two.

Since no clear preference was indicated by the chi-square test, the confidence limits predicted by each distribution were compared. The sine transformation indicated the narrowest confidence interval in five of the eight cases, arctangent in two, and logistic in one. Although the gaussian never predicted the smallest confidence band, the difference between it and the smallest never exceeded four percentage points and the average difference

was less than two percent. Furthermore, the difference between means was only about 1.6%, clearly within the bounds of experimental error.

In summary, the three alternative distributions do indeed verify the results of the probit analysis but do not indicate any preference for one of these over the gaussian.

The data for the retinal burn thresholds are shown to be normally distributed; therefore, a statistical analysis is performed on the retinal burn thresholds. This analysis involves determining the mean retinal burn threshold, $\bar{X}$, for irradiations by the radiation from a laser operating in a given condition (single or repetitive pulse). The standard deviation, σ, is then determined. The 95% confidence interval is computed using the relations $\bar{X} - 1.96\,\sigma/\sqrt{n} \leq \bar{X} \leq \bar{X} + 1.96\,\sigma/\sqrt{n}$ where n is the number of eyes used to determine $\bar{X}$. Thirty eyes were used for the laser operating condition and this is a practical number from the amount of time necessary to make measurements and to obtain valid results. Thirty observations are sufficient to yield statistically valid results. Since the precision in determining, $\bar{X}$, varies inversely as the $\sqrt{n}$, it would be impractical from time and cost considerations to increase the precision. For the precision to be increased by a factor of ten would require retinal burn threshold data from 3,000 eyes for radiation from a laser in a given operating condition.

84